atmosphere

MDPI

Article

# Global Atmospheric $CO_2$ Concentrations Simulated by GEOS-Chem: Comparison with GOSAT, Carbon Tracker and Ground-Based Measurements

**Yingying Jing [1,2], Tianxing Wang [2,*], Peng Zhang [1], Lin Chen [1], Na Xu [1] and Ya Ma [3]**

[1] National Satellite Meteorological Center, China Meteorological Administration (NSMC/CMA), Beijing 100081, China; jingyy@radi.ac.cn (Y.J.); zhangp@cma.gov.cn (P.Z.); chenlin@cma.gov.cn (L.C.); xuna@cma.gov.cn (N.X.)

[2] State Key Laboratory of Remote Sensing Science, Institute of Remote Sensing and Digital Earth, Chinese Academy of Sciences, Beijing 100101, China

[3] Chinese Academy for Environmental planning, Beijing 100012, China; maya@caep.org.cn

* Correspondence: wangtx@radi.ac.cn; Tel.: +86-10-6480-7981

Received: 23 February 2018; Accepted: 4 May 2018; Published: 7 May 2018


**Abstract:** Accurate quantification of the distribution and variability of atmospheric $CO_2$ is crucial for a better understanding of global carbon cycle characteristics and climate change. Model simulation and observations are only two ways to globally estimate $CO_2$ concentrations and fluxes. However, large uncertainties still exist. Therefore, quantifying the differences between model and observations is rather helpful for reducing their uncertainties and further improving model estimations of global $CO_2$ sources and sinks. In this paper, the GEOS-Chem model was selected to simulate $CO_2$ concentration and then compared with the Greenhouse Gases Observing Satellite (GOSAT) observations, CarbonTracker (CT) and the Total Carbon Column Observing Network (TCCON) measurements during 2009–2011 for quantitatively evaluating the uncertainties of $CO_2$ simulation. The results revealed that the $CO_2$ simulated from GEOS-Chem is in good agreement with other $CO_2$ data sources, but some discrepancies exist including: (1) compared with GOSAT retrievals, modeled $XCO_2$ from GEOS-Chem is somewhat overestimated, with 0.78 ppm on average; (2) compared with CT, the simulated $XCO_2$ from GEOS-Chem is slightly underestimated at most regions, although their time series and correlation show pretty good consistency; (3) compared with the TCCON sites, modeled $XCO_2$ is also underestimated within 1 ppm at most sites, except at Garmisch, Karlsruhe, Sodankylä and Ny-Ålesund. Overall, the results demonstrate that the modeled $XCO_2$ is underestimated on average, however, obviously overestimated $XCO_2$ from GEOS-Chem were found at high latitudes of the Northern Hemisphere in summer. These results are helpful for understanding the model uncertainties as well as to further improve the $CO_2$ estimation.

**Keywords:** GEOS-Chem model; GOSAT satellite; CarbonTracker; $XCO_2$

## 1. Introduction

As one of the most important anthropogenic greenhouse gases, the $CO_2$ concentration in the Earth's atmosphere has increased by 40% since pre-industrial times because of human activities [1,2]. Global warming caused by atmospheric $CO_2$ concentrations has gained much attention from climate scientists throughout the world [3,4]. An increased knowledge of the carbon cycle is necessary to predict and mitigate climate change [3,4]. Thus, it is extremely important to accurately quantify the distribution and variability of the global $CO_2$ sources and sinks [4]. Model simulation and observations provide two effective ways to quantitatively estimate $CO_2$ fluxes and concentrations with high accuracy, but the existing in situ measurements of atmospheric $CO_2$ are sparse and even absent

in some regions (e.g., oceans and polar regions) so that large uncertainties exist in the estimation of global $CO_2$ sources/sinks if only using ground-based data [5,6]. Satellite remote sensing provides an advantageous technique to derive the $CO_2$ column-averaged dry air mole fractions ($XCO_2$) for atmospheric inversions on the global and regional scales.

Currently, the Scanning Imaging Absorption Spectrometer for Atmospheric Chartography (SCIAMACHY) from Europe [7], the Greenhouse gases Observing Satellite (GOSAT) from Japan [8], the Orbiting Carbon Observatory-2 (OCO-2) from the United States of America [9] and the TanSAT from China [10] are four typical satellite sensors that can derive $XCO_2$ with significant sensitivity in the boundary layer [7]. Among these instruments, SCIAMACHY mainly measures the global trace gases in the troposphere and stratosphere, including $CO_2$ and $CH_4$ [7], but unfortunately, it has been lost since 2012. The GOSAT as well as the recently launched OCO-2 and TanSAT are specifically designed to accurately estimate atmospheric $CO_2$ and $CH_4$ [8,9]. Moreover, $CO_2$ retrieval algorithms have also been developed based on these instruments, for example, the NASA's Atmospheric $CO_2$ Observations from Space (ACOS) team has applied the OCO retrieval algorithm to the GOSAT Level 1B data [6,11] to produce $XCO_2$ data (hereinafter called GOSAT/ACOS $XCO_2$). These $XCO_2$ data from satellite are very useful to improve estimations of $CO_2$ concentrations and further constrain the model simulations, thereby reducing uncertainties of $CO_2$ sources and sinks. However, due to cloud contamination and limitations of observation modes, the available data number of $XCO_2$ retrievals is very limited [12,13]. Morino et al. [14] pointed out that only about 10% of the GOSAT data points can be used for the $XCO_2$ retrievals. Consequently, these limited $CO_2$ observations could bring additional uncertainties into atmospheric inversion models [15].

Model simulation is another essential tool to quantify the spatio-temporal characteristics of $CO_2$ concentrations and fluxes. Unlike limited satellite observations, it can provide full-coverage atmospheric $CO_2$ concentrations on a global scale. In early studies, two-dimensional transport models were frequently used to estimate the distribution of $CO_2$ fluxes [16], while, in recent decades, three-dimensional (3-D) models have been developed to estimate the distribution as well as interannual variations of $CO_2$ fluxes [16]. Considering the large differences between models, robust estimation of model transport error has become a serious concern [17]. TransCom 3 found that the significant source of uncertainty in $CO_2$ inversion calculations was mainly due to the $CO_2$ flux inventories in transport models by intercomparing $CO_2$ inversion differences among 17 different models [16]. Chevallier et al. emphasized that the uncertainties in models probably limits the utility of the model system for further carbon cycle research [17].

To better estimate the uncertainty in $CO_2$ model inversion, several studies have also assessed the differences between observations and models [15,18,19]. Li et al. [18] compared the differences of atmospheric $CO_2$ concentration in East Asia between the Community Multiscale Air Quality Modeling System (CMAQ) and GOSAT observations to evaluate the uncertainties in model simulation. Saito et al. [20] reported that the latitude-time variations of $XCO_2$, $CH_4$ and $N_2O$ and the transport processes in troposphere and stratosphere were well modeled by an atmospheric general circulation model (AGCM)-based chemistry-transport model (ACTM), which was confirmed through comparisons to TCCON (Total Carbon Column Observing Network). Particularly, GEOS-Chem, as a global 3-D chemical transport model, which plays an important role in characterizing the distribution and variability of global atmospheric $CO_2$ [21], has also been evaluated using surface carbon dioxide monitoring network, aircraft, and satellite observations. For example, Feng et al. [22] evaluated the GEOS-Chem model using GLOBALVIEW, CONTRAIL aircraft and AIRS satellite data. Lindqvist et al. [23] compared the seasonal cycle of ACOS retrievals with the University of Edinburgh model (assimilating two GOSAT retrievals into GEOS-Chem, referred as UoE) in the Northern Hemisphere. Recently, Zhang et al. [24] modeled the HASM $XCO_2$ by fusing the TCCON measurements with GEOS-Chem $XCO_2$ model and compared them with satellite observation. These studies have compared the differences of atmospheric $CO_2$ between GEOS-Chem and other observations in terms of spatial variation, regional bias and latitudinal gradient by seasons. However, the $CO_2$ characteristics of

GEOS-Chem model simulation (e.g., seasonal cycle amplitude as well as model errors, especially $CO_2$ overestimation in the high latitudes in summer) have not been fully investigated and inter-compared with multi-source $CO_2$ data. These inter-comparisons are quite important to quantitatively evaluate model uncertainties and improve the $CO_2$ flux estimate in GEOS-Chem. Therefore, it is necessary to further compare the $CO_2$ characteristics from GEOS-Chem with multi-source $CO_2$ data including observations and other model results to understand uncertainties of $CO_2$ simulation.

For this reason, the overall objective of this study was to simulate atmospheric $CO_2$ using GEOS-Chem and inter-compare the characteristics of $CO_2$ simulation with GOSAT/ACOS $XCO_2$ data, CarbonTracker $CO_2$ modeling system and TCCON site measurements during the years of 2009–2011. The remainder of this paper is organized as follows: Section 2 describes the data and models used in this study; Section 3 introduces the methods to compare the simulated $XCO_2$ from GEOS-Chem and other $CO_2$ data with the results presented in Section 4 along with the comparisons between $XCO_2$ from GEOS-Chem and that of GOSAT/ACOS, CarbonTracker as well as TCCON measurements. The results are discussed in Section 5 and the conclusions are presented in Section 6.

## 2. Data and Models

### *2.1. Datasets*

#### 2.1.1. GOSAT $XCO_2$ Observations

The GOSAT, the first satellite specifically used to accurately monitor $CO_2$ and $CH_4$ [8], was successfully launched on 23 January 2009. It includes a Thermal and Near-infrared Sensor for Carbon Observation Fourier Transform Spectrometer (TANSO-FTS, JAXA, Tokyo, Japan) and a Cloud and Aerosol Imager (CAI, JAXA, Tokyo, Japan). TANSO-FTS mainly measures greenhouse gases in both the Short-Wave InfraRed (SWIR) region (0.76, 1.6 and 2.0 μm) and a wide Thermal InfraRed (TIR) band (5.5–14.3 μm) at a spectral resolution of 0.2 $cm^{-1}$ [8]. TANSO-CAI monitors the clouds and aerosols within the TANSO-FTS's field of view [8]. In recent years, some $CO_2$ retrieval algorithms, e.g., NIES [25], ACOS [6], and UOL-FP [26] have been developed based on the GOSAT satellite. Operational GOSAT/ACOS $CO_2$ products from the NASA's Atmospheric $CO_2$ Observations from Space team have been released and are publicly available. Currently, the version 7.3 of the GOSAT/ACOS $XCO_2$ L2 data [27] is the newest one. Considering the potential deficiencies in M-gain and ocean glint retrievals, only the H-gain land data of GOSAT/ACOS are used in this study. Before incorporating GOSAT/ACOS $XCO_2$ data in this study, data filtering and bias corrections recommended by GOSAT/ACOSv7.3 data users guide [27] were applied for scientific purpose.

#### 2.1.2. Total Carbon Column Observing Network (TCCON) $XCO_2$ Measurements

The Total Carbon Column Observing Network (TCCON) is a global network of ground-based Fourier transform spectrometers that measure atmospheric columns of the gases $CO_2$, CO, $CH_4$, $H_2O$ and others [28–30]. Wunch et al. [28] compared the $XCO_2$ data retrieved from TCCON with integrated aircraft profiles and found an accuracy of approximately 1 ppm in these data. TCCON provides critical ground-based data for validation and bias correction of retrieved $CO_2$ from satellites [28,29], e.g., the calibration of ACOS $XCO_2$ retrievals from GOSAT [11]. In this study, TCCON $XCO_2$ retrievals of the newest GGG2014 version at fourteen sites during January 2009–December 2011 were used to evaluate $XCO_2$ results from the GEOS-Chem model. Sites selected for this study are: Lamont [31], Park Falls [32,33], Bialystok [34,35], Orleans [36,37], Garmisch [38,39], Bremen [40], Sodankylä [41,42], Ny-Ålesund, Izaña [43], Eureka [44], Karlsruhe [45] sites located in the Northern Hemisphere (NH), Wollongong [46], Darwin [47,48], and Lauder [49] sites located in the Southern Hemisphere (SH), were used in this study.

### *2.2. Model Description*

#### 2.2.1. GEOS-Chem Model Description

GEOS-Chem is a global three-dimensional (3-D) chemical transport model (CTM) driven by assimilated meteorological fields from the Goddard Earth Observing System (GEOS-5) of the NASA Global Modeling and Assimilation Office [50]. The original GEOS-Chem $CO_2$ simulation was developed by Suntharalingam et al. [51]. Nassar et al. [21] have completed a major update of $CO_2$ simulations of GEOS-Chem model, which improved the $CO_2$ flux inventories and added $CO_2$ emissions from international shipping and aviation. In this study, the GEOS-Chem model (v9-02) was used to simulate global atmospheric $CO_2$ from 2005 to 2011.

Since the setting of initial $CO_2$ concentration has a significant impact on the simulated results, it is necessary to select the appropriate $CO_2$ concentration to initialize the model. In this study, the $CO_2$ concentration on January 2005 was initially set as 375 ppm on the global scale similar to Nassar et al. [21]. Four years after initialization, a more reasonable $CO_2$ distribution pattern was generated to again drive the model calculation. Finally, the global atmospheric $CO_2$ distribution is effectively simulated and available for the years of 2009–2011 in this study. The simulated $CO_2$ included 47 vertical levels with a horizontal grid resolution of $2^\circ \times 2.5^\circ$ latitude/longitude. The time period of $CO_2$ simulation is set at 13:00 $\pm$ 2 h local time to match the overpass time of the GOSAT satellite.

The input surface $CO_2$ fluxes include: (1) fossil fuel burning and cement manufacture from an inventory developed at the Carbon Dioxide Information and Analysis Centre (CDIAC) [52]; (2) Monthly biomass burning from the third version of the Global Fire Emission Database (GFEDv3) [53]; (3) Terrestrial biospheric exchange in the model including two components: a balanced biosphere computed by the CASA biospheric model and the residual annual terrestrial exchange obtained by inverse modeling in the TransCom 3 project [21,54,55]. The CASA Net Ecosystem Productivity (NEP) output is used as Net Ecosystem Exchange (NEE) in the GEOS-Chem model simulation [21]. It should be noted that these balanced biospheric fluxes contribute no net annual uptake of $CO_2$, but they make the greatest contribution to the seasonal cycle of atmospheric $CO_2$ over most of the globe with the largest impact in the Northern Hemisphere [21]. The residual annual terrestrial exchange is based on the TransCom $CO_2$ inversion results adjusted with GFEDv2 fire emissions and account for the total annual sum of biospheric uptake and emission of $CO_2$ [21]; (4) The ocean fluxes of $CO_2$ from Takahashi et al. [56]. Other fossil fuel emissions from international shipping and aviation have also been included in the GEOS-Chem simulation [21]. The $CO_2$ module and sources/sinks inventories is described in detail by Nassar et al. [21].

#### 2.2.2. CarbonTracker

CarbonTracker (CT) is a $CO_2$ data assimilation system built by the National Oceanic and Atmospheric Administration (NOAA, Silver Spring, MD, USA), Earth System Research Laboratory (ESRL, Boulder, CO, USA) and uses the Transport Model 5 (TM5) offline atmospheric tracer transport model to propagate surface emissions [57]. CarbonTracker $CO_2$ profiles of CT2013B and CT2016 version during 2009–2011 were collected for comparison with modeled $CO_2$ of the GEOS-Chem model in this study. The CT provides global $CO_2$ profiles of 25 vertical levels with $3^\circ \times 2^\circ$ longitude/latitude grids and 3-h temporal resolution [58].

The input $CO_2$ fluxes used in CarbonTrakcer contain: (1) two fossil fuel emissions from Miller and ODIAC datasets. These two datasets provide similar global emissions for each year, but differ in spatial and temporal distribution [59]; (2) biomass burning based on CASA-GFED [59], which is similar to that used in GEOS-Chem; (3) two terrestrial biosphere flux; for CT2013B from CASA-GFEDv2 and GFEDv3; for CT2016 from GFEDv4 and GFED_CMS. It reported that CASA-GFEDv3 product has a smaller seasonal cycle than the older CASA-GFEDv2 [59]; (4) The ocean fluxes of $CO_2$ from Takahashi et al. [56] and ocean inversions (OIF) [59,60] results; (5) assimilation of in situ observations including tall towers, flasks sampled by the NOAA Cooperative Air Sampling Network, and continuous measurements

from partners [59]. A comparison of $CO_2$ input parameters among CT2013B, CT2016 and GEOS-Chem is shown in Table 1.

**Table 1.** Comparison of resolution, input surface $CO_2$ fluxes, transport models and assimilated observation Among CT2013B, CT2016 and GEOS-Chem.

| Models | Resolution | Biospheric Flux | Fossil Fuel | Transport Model | Biomass Burning | Assimilated Obs |
|---|---|---|---|---|---|---|
| GEOS-Chem | 2° × 2.5° lat/lon ×47 | CASA/GFEDv3 | CDIAC | GEOS5 | CASA/GFEDv3 | no |
| CT2013B | 2° × 3° lat/lon ×25 | CASA/GFEDv3 and GFEDv2 | CDIAC and Miller | TM5 | CASA/GFEDv3 and GFEDv2 | in situ data |
| CT2016 | 2° × 3° lat/lon ×25 | CASA/GFEDv4 and GFED_CMS | CDIAC and Miller | TM5 | CASA/GFEDv4 and GFED_CMS | in situ data |

## 3. Methodology

It is well known that different $CO_2$ products cannot be directly compared with each other as a result of their different data sources and samplings methods. For example, $CO_2$ products retrieved from GOSAT/ACOSv7.3 are $CO_2$ column-averaged dry air mole fraction ($XCO_2$) concentrations, while the modeled results from GEOS-Chem are $CO_2$ profiles with 47 vertical layers. Considering these discrepancies, an adjustment must be conducted before comparing them with each other. In this study, the model-simulated $CO_2$ profiles were converted to $XCO_2$ by using averaging kernel and a priori profile of GOSAT/ACOS according to Rodgers and Connor [61] for comparing with GOSAT observations. The adjustment equation is expressed as follows:

$$XCO_2^m = XCO_2^a + \sum_j h_j a_j (y_m - y_a)_j \quad (1)$$

where $XCO_2{}^m$ refers to the transformed model $XCO_2$, $XCO_2{}^a$ is the GOSAT/ACOS a priori $XCO_2$, $h$ denotes pressure weighting function, $a$ is the GOSAT/ACOS v7.3 column averaging kernel, $y_m$ is the simulated $CO_2$ vertical profile, $y_a$ is the GOSAT/ACOS v7.3 a priori $CO_2$ profile.

The detailed adjustment method was performed as follows. First, the GEOS-Chem $CO_2$ profiles were extracted and interpolated to the corresponding time and locations of the GOSAT/ACOS v7.3 $XCO_2$ data. After interpolation according to the GOSAT/ACOS pressure levels, the simulated $CO_2$ profiles have the same layers as a priori $CO_2$ profiles of the GOSAT/ACOS. Then, the interpolated $CO_2$ profiles from the GEOS-Chem model are convolved with the averaging kernel of GOSAT/ACOS to obtain $XCO_2$ as in Equation (1). These transformed $XCO_2$ from the GEOS-Chem model are then compared with GOSAT/ACOSv7.3 $XCO_2$ data in terms of their spatial and temporal characteristics as well as time series variations.

Furthermore, modeled $CO_2$ from both GEOS-Chem and CarbonTracker are $CO_2$ profiles with different vertical levels (e.g., GEOS-Chem for 47 layers and CarbonTracker for 25 layers). To better compare them with each other on the global scale, their $CO_2$ profiles are uniformly transformed to $XCO_2$ according to the weighting pressure-averaged method described by O'Dell et al. [6]:

$$XCO_2 = \mathbf{h}^T \hat{\mathbf{u}} \quad (2)$$

where $\hat{\mathbf{u}}$ is the $CO_2$ profiles from the CarbonTracker or GEOS-Chem model on discrete pressure levels and $\mathbf{h}$ is the pressure weighting function. The specific conducted method of $\mathbf{h}$ is described in O'Dell et al. [6].

In addition, to compare modeled $CO_2$ from GEOS-Chem with TCCON $XCO_2$ measurements, the GEOS-Chem $CO_2$ profiles should be transferred to $XCO_2$ by using TCCON column averaging kernels and a priori $CO_2$ profiles [28,62,63]. The averaging kernel correction formula is similar to Equation (1). Here, the model-simulated $CO_2$ profiles are extracted and integrated to $XCO_2$ within ±2.5° latitude and ±2.5° longitude of each TCCON site. $XCO_2{}^m$ denotes the integrated

$XCO_2$ from GEOS-Chem; $XCO_2^a$ is the TCCON a priori $XCO_2$; $h$ is pressure weighting function; $a$ is the TCCON column averaging kernel, which is a function of pressure and the solar zenith angle; $y_m$ is the simulated $CO_2$ profile; $y_a$ is the TCCON a priori $CO_2$ profile. The detailed method is described in Wunch et al. [28].

## 4. Results and Discussion

### *4.1. Comparison with GOSAT/ACOS $XCO_2$ Retrievals*

Satellite measurements (e.g., GOSAT) can provide spatiotemporal distribution characteristics of global atmospheric $CO_2$ and have the potential to improve model flux estimation. Motivated by this, we compare modeled $CO_2$ from GEOS-Chem with GOSAT/ACOSv7.3 retrievals over land in this study to evaluate the uncertainties of $CO_2$ simulations. However, atmospheric $CO_2$ data from GOSAT/ACOS are $XCO_2$ concentrations, while those from the GEOS-Chem model are $CO_2$ profiles with 47 vertical levels. For comparison between them, the model-simulated $CO_2$ profiles were transformed to $XCO_2$ according to the time and location of GOSAT/ACOS retrievals based on the method in Section 3. It is noted that the $CO_2$ data used in this study during the period of March 2010 to February 2011, are divided by seasons in this study: spring (MAM, March–May), summer (JJA, June–August), autumn (SON, September–November), and winter (DJF, December 2010–February 2011). From Figure 1, obviously sparse spatial coverage is observed in GOSAT/ACOSv7.3 $XCO_2$ distribution because of some factors, e.g., cloud contamination or limitations of GOSAT observation modes as well as solar zenith angles [13,26].

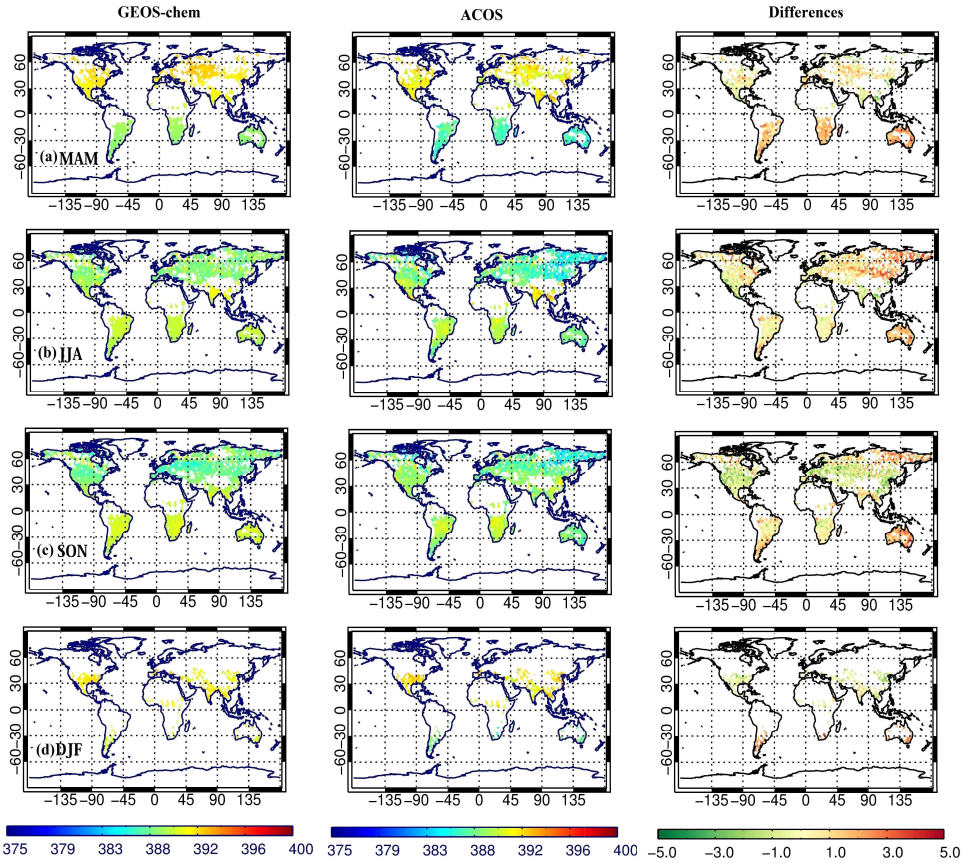


**Figure 1.** Comparison of $XCO_2$ simulated with GEOS-Chem and GOSAT/ACOSv7.3 $XCO_2$ products during March 2010–February 2011. Seasonal averaged $XCO_2$ concentrations are shown for GEOS-Chem, GOSAT/ACOSv7.3 and their differences (GEOS-Chem −ACOS): (**a**): MAM; (**b**): JJA; (**c**): SON; (**d**): DJF. Unit: ppm.

Figure 1 also reveals that seasonal variations of $XCO_2$ in the NH are apparent for the GEOS-Chem model and GOSAT/ACOSv7.3, with the higher $CO_2$ concentrations occurred in MAM and DJF as well as the lower ones in JJA and SON. There was no significant seasonal variation found in the SH. The cause of these significant seasonal variations in the NH may be mainly that strong photosynthesis by vegetation in JJA and SON results in the decay of the $CO_2$ concentration and winter heating leads to higher $XCO_2$ concentration in MAM and DJF [13,64].

As presented in Figure 1, although the spatial distribution characteristics are consistent between GEOS-Chem and GOSAT/ACOS on the whole, the differences are evident in each season. For example, $XCO_2$ from GEOS-Chem is overestimated relative to that of GOSAT/ACOSv7.3 at many regions, especially in the SH and high latitude region in the NH. However, underestimated $XCO_2$ is found in the middle latitude region of the NH, particularly in SON.

Furthermore, there are consistent latitudinal variations between GEOS-Chem and GOSAT/ACOS v7.3 retrievals in Figure 2. Nevertheless, some discrepancies are obvious between them (GEOS-Chem −GOSAT/ACOS), which vary from 0.2 ppm to 0.78 ppm, with the largest difference (0.78 ppm) in summer. The result in Figure 2 also shows that overestimated $XCO_2$ from GEOS-Chem were found, especially in the SH as well as 55° N–65° N latitude band in JJA, with largest overestimated value point-by-point even up to 2.88 ppm in the 20° S latitude band in winter. However, underestimated $XCO_2$ was observed over tropical region of the NH in MAM and DJF, as well as middle latitude region of NH in JJA and SON. For underestimated $XCO_2$ over tropical region in MAM and DJF, it may be affected by satellite retrieval errors due to tropical cloud during these seasons. This result is also in good agreements with Cogan et al. [26]. Few data is found in the high latitude of the NH for GOSAT/ACOS $XCO_2$ in DJF due to the effect of large solar zenith angles in GOSAT observation. In addition, it can also be seen from Figure 2 that the standard deviation of GOSAT/ACOSv7.3 is relatively larger than GEOS-Chem, which indicates the larger discrete variation of GOSAT/ACOS retrievals.

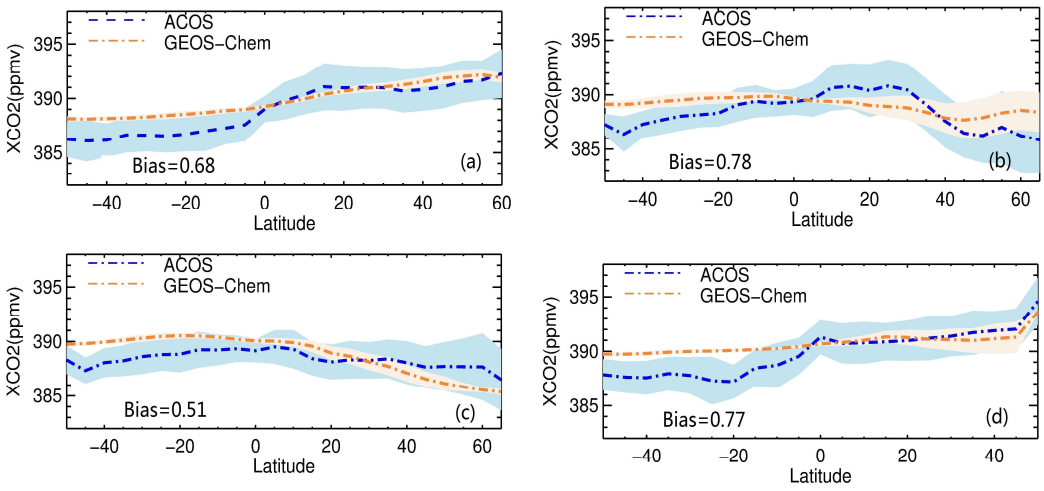


**Figure 2.** $XCO_2$ concentrations of GOSAT/ACOSv7.3 and GEOS-Chem averaged over 5° latitude bins during March 2010–February 2011: (**a**) MAM; (**b**) JJA; (**c**) SON; (**d**) DJF. Blue lines denote the latitudinal mean GOSAT/ACOSv7.3 $XCO_2$ data, with the light blue envelope representing their standard deviation. Orange line and light orange envelope denotes the latitudinal mean GEOS-Chem $XCO_2$ concentrations and their corresponding standard deviation.

The seasonal correlation coefficients of $XCO_2$ between GOSAT/ACOS and GEOS-Chem in Figure 3 show that best correlation ($R$ = 0.80) is found in MAM and the poorest correlation ($R$ = 0.52) in SON. Cogan et al. [26] also found that GEOS-Chem (v08-02) showed highest correlation with GOSAT observation (UoL-FP retrievals) in MAM.

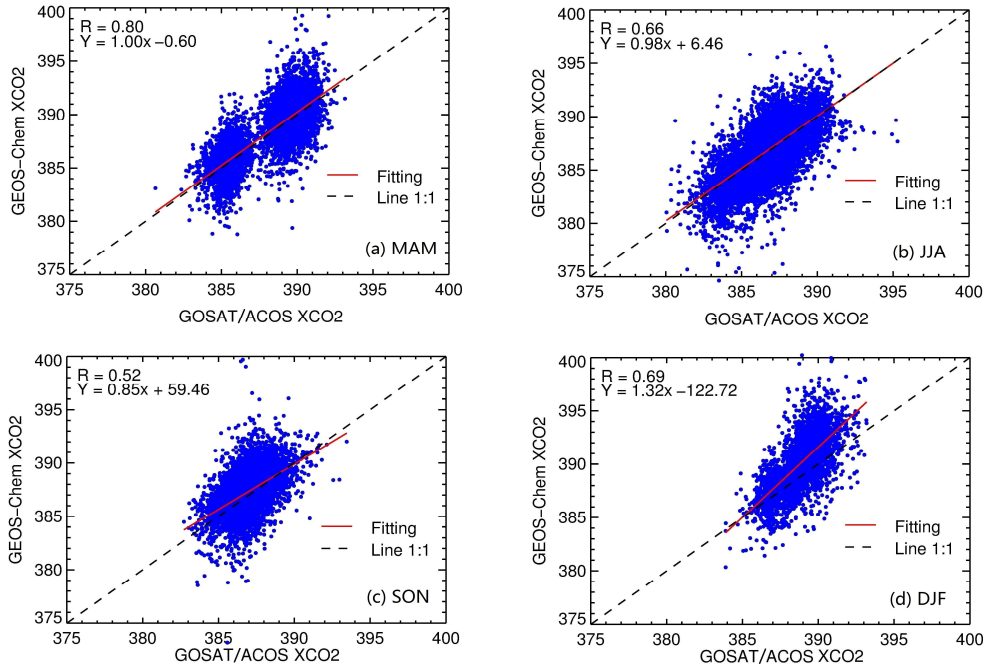


**Figure 3.** Scatter plots of $XCO_2$ retrievals of GOSAT/ACOS v7.3 versus $XCO_2$ simulation from GEOS-Chem during March 2010–February 2011. (**a**)–(**d**) indicate MAM, JJA, SON and DJF respectively. Unit: ppm.

In addition, as shown in Figure 4, the time series variations of $XCO_2$ from GEOS-Chem in the NH during April 2009–December 2011 show good agreement with those of GOSAT/ACOSv7.3, but monthly averaged $XCO_2$ in the SH is obviously overestimated by GEOS-Chem (even up to 2.5 ppm in April 2011). Overall, the average bias between GEOS-Chem and GOSAT/ACOS is 0.78 ppm (GEOS-Chem −GOSAT/ACOS) on the global land during April 2009–December 2011. From Figure 4, in the NH, the $CO_2$ seasonal cycle dependence of GOSAT/ACOSv7.3 is stronger than GEOS-Chem in JJA.

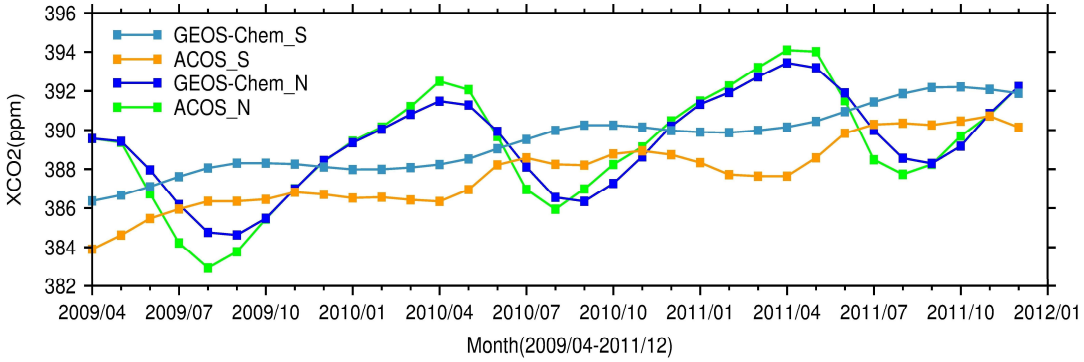


**Figure 4.** The time series variations of monthly averaged $XCO_2$ for April 2009–December 2011 in the NH and SH between GOSAT/ACOS and GEOS-Chem. The green line denote the GOSAT/ACOS $XCO_2$ retrievals in the NH and the orange one is in the SH; the two blue lines refers to the $XCO_2$ simulated from GEOS-Chem in the NH and SH respectively.

Monthly averaged $XCO_2$ result in Table 2 and time series variations of the NH in Figure 4 also reveal the largest difference (1.2 ppm) between GEOS-Chem and GOSAT/ACOS found in JJA. This phenomenon coincides with the seasonal drawdown of $XCO_2$ and therefore may be connected

to the biospheric fluxes in the GEOS-Chem model. Li et al. [18] stated that the uncertainty in the terrestrial biosphere has a strong effect on $CO_2$ simulations in summer.

**Table 2.** Statistics of the number of $XCO_2$ data (N), standard deviation (STD) and averaged biases (Bias) for GEOS-Chem (G-C), GOSAT/ACOS (G-A for GEOS-Chem −ACOS) over the global land during March 2010–February 2011. Unit: ppm.

| Month | Num | G-C | STD $^{G-C}$ | ACOS | STD $^{A}$ | Bias $^{G-A}$ |
|---|---|---|---|---|---|---|
| 03/2010 | 2286 | 389.74 | 1.48 | 389.33 | 2.90 | 0.41 |
| 04/2010 | 2424 | 390.01 | 1.72 | 389.81 | 3.54 | 0.26 |
| 05/2010 | 3339 | 389.82 | 1.46 | 389.37 | 3.14 | 0.46 |
| 06/2010 | 4429 | 389.44 | 0.65 | 388.87 | 2.11 | 0.58 |
| 07/2010 | 5095 | 388.85 | 0.94 | 387.80 | 2.45 | 1.05 |
| 08/2010 | 5098 | 388.42 | 1.80 | 387.20 | 2.23 | 1.23 |
| 09/2010 | 4481 | 388.07 | 2.02 | 387.52 | 1.81 | 0.55 |
| 10/2010 | 3880 | 388.32 | 1.57 | 388.43 | 1.80 | −0.11 |
| 11/2010 | 3167 | 389.08 | 1.02 | 389.08 | 1.82 | 0.00 |
| 12/2010 | 2598 | 390.14 | 0.66 | 389.96 | 1.98 | −0.17 |
| 01/2011 | 2232 | 390.98 | 0.73 | 390.74 | 2.44 | 0.25 |
| 02/2011 | 1908 | 391.21 | 1.05 | 391.21 | 2.80 | 0.24 |

Additionally, the result from Table 2 indicates that monthly averaged biases (GEOS-Chem—GOSAT/ACOS) during March 2010–December 2011 ranging from −0.11 ppm to 1.23 ppm. However, Lei et al. [19] found that the bias between GEOS-Chem and GOSAT (NIES algorithm) $XCO_2$ could be up to around 3.3 ppm. This discrepancy between our study and Lei et al. [19] could be due to different retrieval algorithms of GOSAT and different version of GEOS-Chem model simulation.

From Table 2, the monthly averaged standard deviation of GOSAT/ACOSv7.3 $XCO_2$ is relatively larger (even up to 3.5 ppm) than that of $XCO_2$ simulated from GEOS-Chem, indicating the more discrete variation of GOSAT/ACOSv7.3 $XCO_2$ than those of GEOS-Chem. This phenomenon is similar to the result shown in Figure 2. The reason for more discrete variations of GOSAT/ACOS $XCO_2$ may be that, on the one hand, the GEOS-Chem model is not better to capture complicated dynamic variations of $XCO_2$ than satellite observations [15]. On the other hand, the retrieval errors on satellite observations [23,26] could lead to large uncertainties in the GOSAT/ACOSv7.3 $XCO_2$.

### *4.2. Comparison with CarbonTracker $XCO_2$*

Satellite $XCO_2$ retrievals are useful in analyzing $XCO_2$ variability and informing carbon cycle science. Nonetheless, their limited observations probably lead to uncertainties in further interpreting their scientific significance [65]. Unlike satellite $XCO_2$ retrievals, model simulations (e.g., GEOS-Chem) can provide full-coverage maps of $CO_2$ concentrations on the global or regional scale. To further compare the differences between GEOS-Chem and CarbonTracker, global $CO_2$ profiles from GEOS-Chem, CT2013 and CT2016 are converted to $XCO_2$ using Equation (2) in this section. In view of a high similarity of input surface fluxes in GEOS-Chem and CT2013B, we mainly analyze the spatial distribution, seasonal correlation and time series variations of $XCO_2$ between GEOS-Chem and CT2013B.

The spatial distribution of $XCO_2$ between GEOS-Chem and CT2013B in Figure 5 indicates that significant seasonal variations of global atmospheric $CO_2$ are found from these two model simulations. The difference (GEOS-Chem −CT2013B) result shows that the seasonal averaged $XCO_2$ of GEOS-Chem is slightly underestimated relative to that of CT2013B at most regions on the global scale, apart from eastern China and middle Africa in MAM, SON and DJF, northern South America as well as high latitude of the NH in JJA. Here, we simply analyze the overestimated effect in these regions. From Figure 6, limited assimilated observation sites for CT2013B are found in these regions, therefore, the assimilated effect of CT2013B is small and not discussed in these regions. From Table 1,

GEOS-Chem used ODIAC as fossil fuel emission input, and CT2013B simultaneously used ODIAC and Miller dataset. CT2013B document [59] reported that large fossil emission differences between ODIAC and Miller datasets were found in eastern China, although ODIAC and Miller have similar global emissions for each year. Overestimated $XCO_2$ from GEOS-Chem over eastern China may be due to the effect of fossil fuel emission inventory differences. For middle Africa and northern South America, overestimated $XCO_2$ from GEOS-Chem is probably related to spatial distribution differences in terrestrial biosphere fluxes between GFED3 and GFED2. These spatial differences between GFED3 and GFED2 were also described by CT2013 document [59]. For more details, please see the CT2013 document [59]. For the high latitude region in the NH, the difference of biosphere fluxes and fossil fuel emission in this region used in GEOS-Chem and CT2013B is very small according to CT2013B document [59], but transport models are different. Therefore, overestimated $XCO_2$ from GEOS-Chem in summer for the high latitudes of NH are likely affected by atmospheric transport and local fluxes.

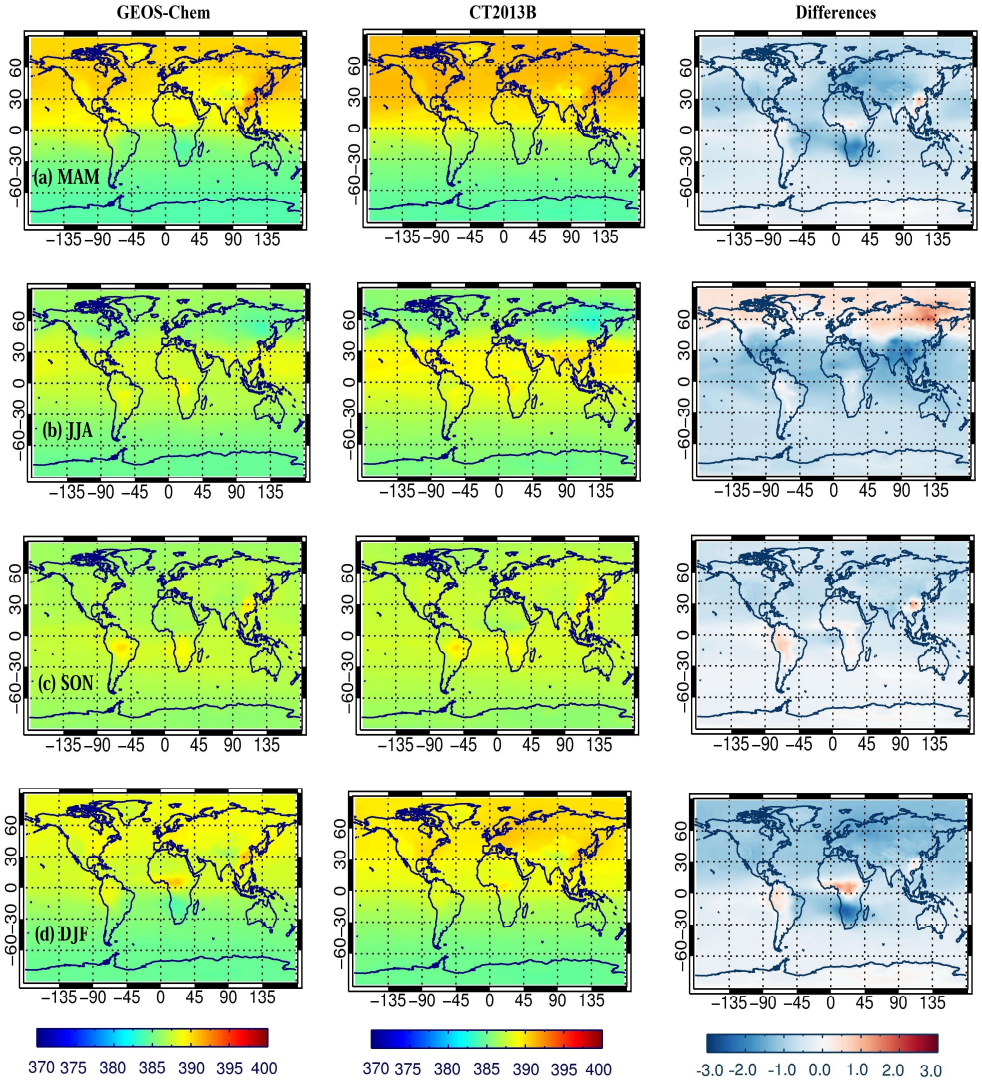


**Figure 5.** Comparison of global $XCO_2$ simulated with GEOS-Chem and CT2013B during March 2010–February 2011. Seasonal averaged $XCO_2$ concentrations are shown for GEOS-Chem, CT2013B and their difference (GEOS-Chem −CT2013B). (**a**) MAM; (**b**) JJA; (**c**): SON; (**d**): DJF. Unit: ppm.

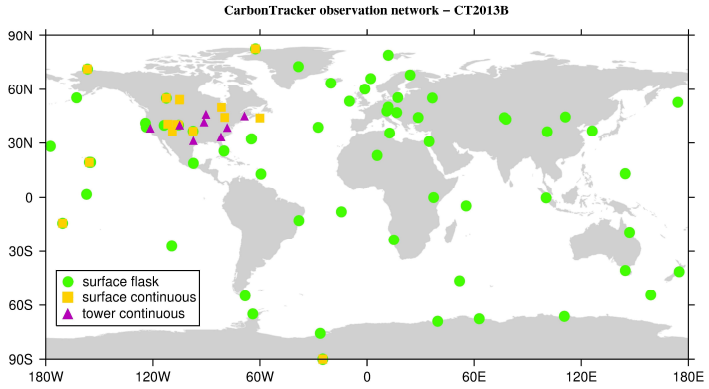


**Figure 6.** The spatial distribution of CT2013B assimilated observational network (source: CarbonTracker website).

The seasonal correlation in Figure 7 shows that the highest correlation of $XCO_2$ (up to 0.98) between GEOS-Chem and CT2013B is found in MAM, with an average bias of −0.59 ppm, while the poorest correlation also reached approximately 0.93 in SON, with the smallest average bias of −0.37 ppm. The $XCO_2$ from these two models show very good correlation for each season on the whole, but remarkably overestimated $XCO_2$ for GEOS-Chem (more than 6 ppm) are found in Figure 7b, which mainly located at high latitude of the NH as shown in Figure 5.

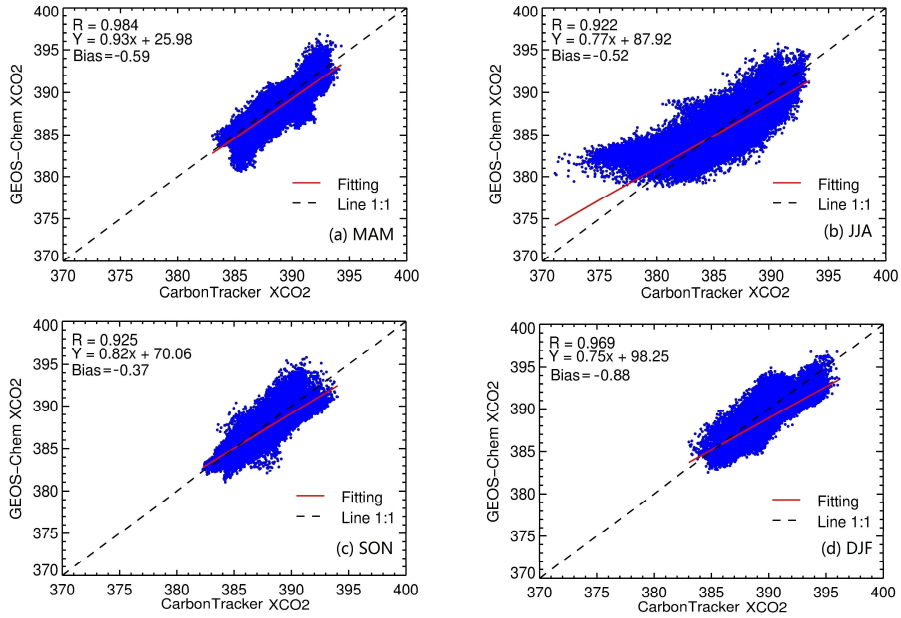


**Figure 7.** Scatter plots of $XCO_2$ from CarbonTracker (CT2013B) versus that of GEOS-Chem during March 2010–February 2011. (**a**)–(**d**) indicate MAM, JJA, SON and DJF respectively. Unit: ppm.

Figure 8 shows that there is good agreement among GEOS-Chem, CT2013B and CT2016 with regard to the seasonal cycle of monthly averaged $XCO_2$ during 2009–2011. As presented in Table 1, both GEOS-Chem and CT2013B use CASA biospheric flux (GFED3 or GFED2) as their input surface flux. Lindqvist et al. [29] reported that biospheric flux is closely connected to seasonal cycle of $CO_2$. Nearly identical time series variation of $XCO_2$ in JJA and SON in Figure 8 between GEOS-Chem and CT2013B are probably influenced by similar biospheric flux components. This result was also reported by Lindqvist et al. [23]. However, CT2013B Document [59] have found that the newer CASA-GFEDv3 product has a smaller seasonal cycle than the older CASA-GFEDv2. Compared with the time series of

CT2013B, the global $XCO_2$ simulated from GEOS-Chem were slightly underestimated on the whole, which may be due to the newer CASA-GFEDv3 biospheric flux used in GEOS-Chem, as well as different transport models or the assimilation of observation data (e.g., GLOBALVIEW data) from CT2013B. Furthermore, the CT2013B show nearly identical variation with the CT2016 due to their similar input surface fluxes and transport models (shown in Table 1). However, due to the difference of biospheric flux version, their seasonal cycle shows a little discrepancies in JJA.

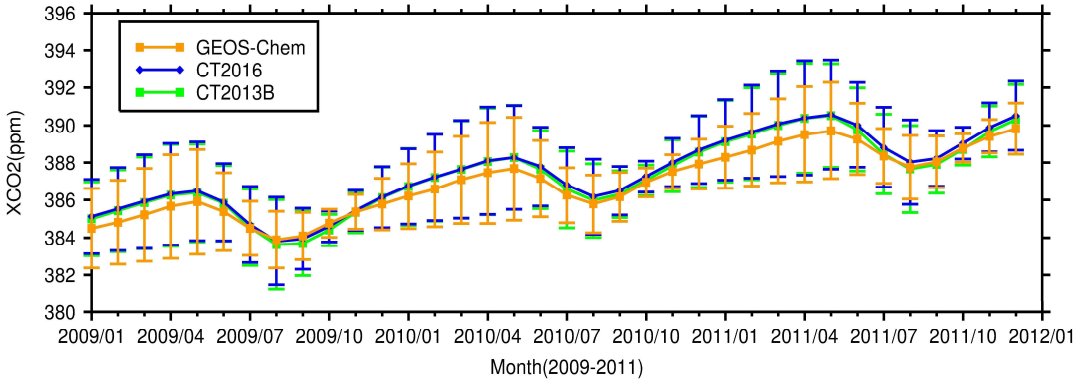


**Figure 8.** The time series variations of monthly averaged $XCO_2$ and standard deviation for 2009–2011 among CT2013B, CT2016 and GEOS-Chem on the global scale. The orange line is the $XCO_2$ simulated from GEOS-Chem; the blue line refers to $XCO_2$ simulated from CT2016; the green line is the $XCO_2$ of CT2013B. Unit: ppmv.

For standard deviation, most of the monthly averaged $XCO_2$ from CT2013B shows a slightly larger discrete variation than the GEOS-Chem model. The larger discrete variation in CT2013B may be due to different transport models, as well as the assimilation of observation data (e.g., GLOBALVIEW data) in the CT2013B.

### *4.3. Comparison with TCCON $XCO_2$ Measurements*

To further validate the GEOS-Chem $CO_2$ simulations, ground-based TCCON measurements during 2009–2011 were used in this study. Since TCCON measurements were $XCO_2$ observations, the model-simulated $CO_2$ profiles need to be first sampled at the location of TCCON observation and integrated to $XCO_2$ by using the TCCON averaging kernels and a priori profiles as described in Section 3. The ground-based $XCO_2$ retrievals from fourteen TCCON sites were compared to the modeled $CO_2$ from GEOS-Chem at around 13:00 $\pm$ 2 h local time.

The comparison result in Figure 9 shows that evident time series variations of $XCO_2$ from the GEOS-Chem model and TCCON sites are observed in the NH sites, e.g., Bialystok, Lamont, Park Falls, Garmisch, and Orleans. No obviously seasonal variations were found in Wollongong, Darwin and Lauder sites of the SH. The $XCO_2$ comparisons in Figure 10 and Table 3 reveal that the model bias at most sites is within $\pm$1.0 ppm, except at Eureka ($-$1.2 ppm). The model bias is relatively smaller in the SH sites (<0.5 ppm) than those in the NH sites (<1.2 ppm). However, relative to GOSAT/ACOS, the model bias is a litter larger in the SH than that in the NH. The result in Figure 10a and Table 3 also indicates that modeled $XCO_2$ from GEOS-Chem are underestimated at most sites, which shows good agreement with the result from comparison with CT2013B. Other studies also reported the underestimated effect of $XCO_2$ in model simulation (e.g., ACTM, TM5 models) [20,66]. However, overestimated $XCO_2$ from GEOS-Chem are found at some sites, including Garmisch (+0.79 ppm), Karlsruhe (+0.03 ppm), Sodankylä (+0.68 ppm) and Ny-Ålesund(+0.37 ppm). As for Garmisch, complex geographical terrain (valleys) at station probably result in model overestimation. For Sodankylä and Ny-Ålesund sites in the far north, model overestimation of $CO_2$ is likely caused by atmospheric transport and local fluxes that has been discussed in Section 4.2 This result is also

similar to the performance of the NIES TM model, which shows a larger bias (+1.22 ppm) for $XCO_2$ over Sodankylä [67].

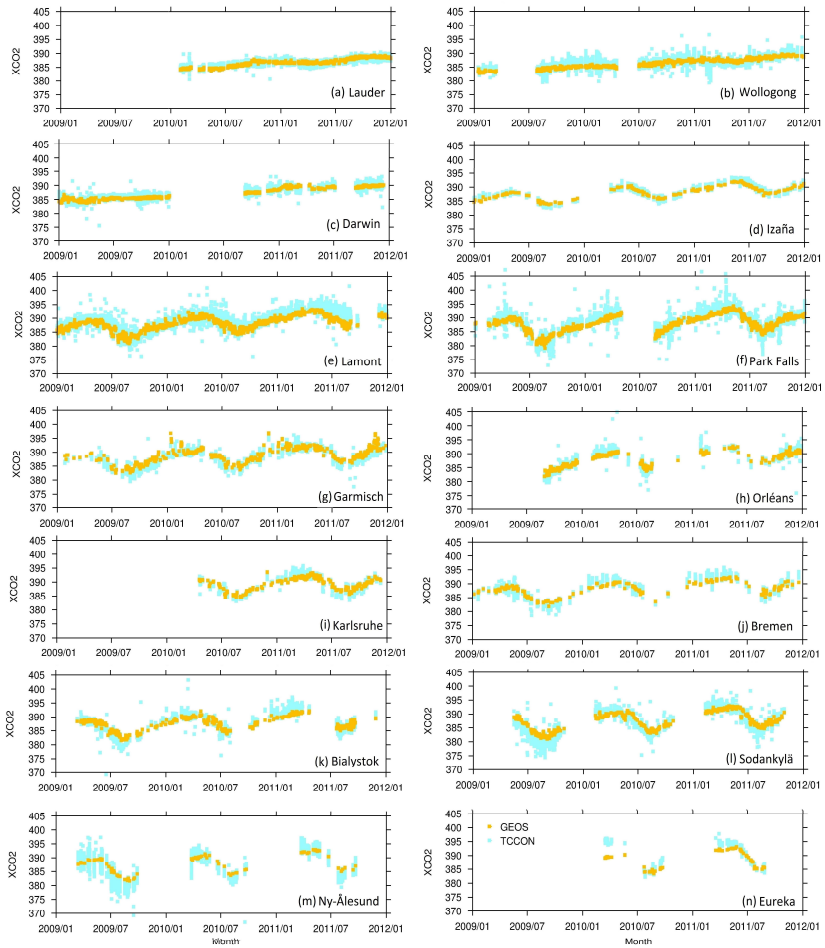


**Figure 9.** Comparison of $XCO_2$ from GEOS-Chem (yellow dots) and ground-based TCCON $XCO_2$ measurements (blue dots) during 2009–2011: (**a**) Lauder; (**b**) Wollongong; (**c**) Darwin; (**d**) Izaña; (**e**) Lamont; (**f**) Park Falls; (**g**) Garmisch; (**h**) Orleans; (**i**) Karlsruhe; (**j**) Bremen; (**k**) Bialystok; (**l**) Sodankylä; (**m**) Ny-Ålesund; (**n**) Eureka.

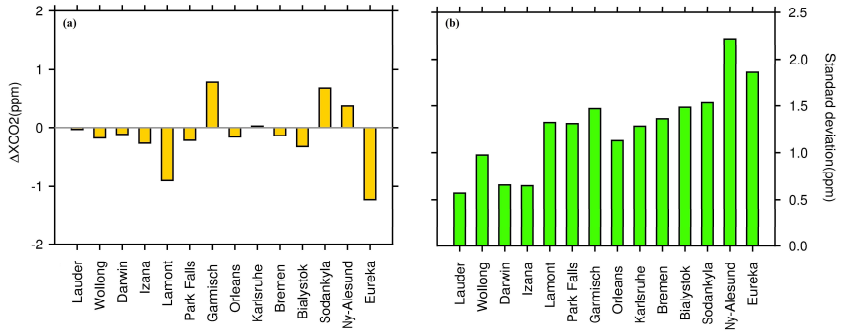


**Figure 10.** Bias and root-mean-square error (RMSE) of GEOS-Chem model vs. TCCON sites in 2010. (**a**) model bias; (**b**) RMSE. Unit: ppm.

**Table 3.** Statistics of number of $XCO_2$ data (N) at TCCON sites, averaged $XCO_2$, correlation coefficient (R), averaged bias (Bias) and root-mean-square error (RMSE) between GEOS-Chem (G-C) and TCCON during 2009–2011.

| Sites | N | TCCON | G-C | R | Bias | RMSE |
|---|---|---|---|---|---|---|
| Lauder (45.04° S,169.68° E) | 28,453 | 387.04 | 386.96 | 0.92 | −0.03 | 0.57 |
| Wollongong(34.41° S, 150.88° E) | 12,546 | 386.66 | 386.48 | 0.83 | −0.18 | 0.98 |
| Darwin (12.42° S, 130.89° E) | 9451 | 386.78 | 386.66 | 0.95 | −0.12 | 0.66 |
| Izaña (28.3° N, 16.5° W) | 4024 | 389.61 | 389.34 | 0.94 | −0.27 | 0.65 |
| Lamont (36.61° N,97.49° W) | 41,176 | 388.79 | 387.91 | 0.90 | −0.90 | 1.32 |
| Park Falls (45.95° N, 90.27° W) | 19,857 | 388.05 | 387.83 | 0.93 | −0.22 | 1.31 |
| Garmisch (47.48° N, 11.06° E) | 7714 | 388.39 | 389.16 | 0.87 | 0.79 | 1.47 |
| Orleans (47.97° N, 2.11° E) | 6934 | 388.30 | 388.13 | 0.90 | −0.16 | 1.13 |
| Karlsruhe (49.1° N, 8.4° E) | 620 | 389.55 | 389.57 | 0.91 | 0.03 | 1.28 |
| Bremen (53.10° N,8.85° E) | 3447 | 388.42 | 388.29 | 0.93 | −0.14 | 1.36 |
| Bialystok (53.23° N,23.03° E) | 11,933 | 388.41 | 388.09 | 0.95 | −0.33 | 1.48 |
| Sodankylä (67.37° N, 26.63° E) | 16,936 | 386.68 | 387.35 | 0.97 | 0.68 | 1.53 |
| Ny-Ålesund (78.92° N, 11.92° E) | 857 | 387.76 | 388.13 | 0.92 | 0.37 | 2.21 |
| Eureka (80.1° N, 86.4° W) | 698 | 389.14 | 387.92 | 0.90 | −1.23 | 1.86 |

As presented in Table 3, $XCO_2$ from GEOS-Chem show strong correlation with the TCCON data ($R > 0.83$), indicating a good representation of transport and fluxes in GEOS-Chem for simulated $CO_2$. However, in the far north (Eureka and Sodankylä, Finland), the result show good correlation ($R > 0.9$) but the model bias is relatively high (>0.5 ppm), which is probably caused by atmospheric transport and local flux in high latitude of the NH. From Figure 10b and Table 3, the root-mean-square error (RMSE) also show small differences between GEOS-Chem and TCCON sites, with the largest RMSE (2.21 ppm) at the Ny-Ålesund site located in the far north. The RMSE is somewhat smaller at the SH stations than most of the NH sites, except Izaña site.

Seasonal biases can affect the seasonal cycle amplitude, and the seasonal cycle is important for biospheric flux attribution [68]. From Figure 11, in MAM and DJF, the modeled $XCO_2$ from GEOS-Chem are underestimated at most sites, except Garmisch and Izaña. However, similar to Figure 10 and Table 3, the overestimated $XCO_2$ occurred at the sites of high latitude of the NH in JJA, especially overestimated seasonal bias more than 1 ppm found at Sodankylä and Ny-Ålesund sites. This comparison result is also consistent with that of GOSAT/ACOS as well as CT2013B and probably related to transport model and local flux in GEOS-Chem.

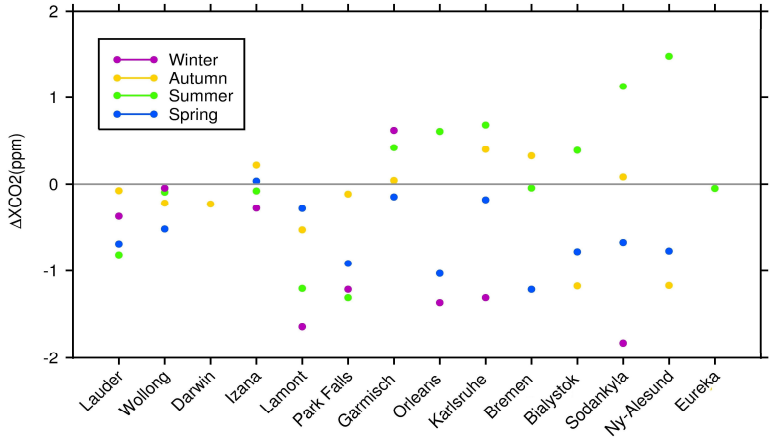


**Figure 11.** Variations of seasonal biases between GEOS-Chem and TCCON sites during March 2010–December 2011: MAM, blue; JJA, green; SON; yellow and DJF, purple.

The seasonal cycle of $XCO_2$ is closely related to the biospheric fluxes that determine the global terrestrial net $CO_2$ sinks [23]. To compare the seasonal cycle of $XCO_2$ from GEOS-Chem and TCCON sites, we use the NOAA fitting software CCGCRV [69] to statistically fit the seasonal cycle and yearly

growth of $XCO_2$. Constrained by short time series or large data gaps, only seven sites in the NH are used to extract the seasonal cycle of $XCO_2$ in this study. It is noted that the detrended seasonal cycle is calculated by removing the long-term trends of $XCO_2$. From Figure 12, the seasonal cycles in GEOS-Chem $XCO_2$ are in good agreement with those of TCCON sites, for example, no apparent mismatches found at the Garmisch, Park Falls and Lamont sites. However, seasonal cycle amplitudes of $XCO_2$ are obviously underestimated by GEOS-Chem at some sites, such as Bialystok, Bremen and Sodankylä sites, which may be due to the biospheric fluxes or transport in model. The result also shows consistency with previous studies, reporting an underestimation of $XCO_2$ peak-to trough amplitudes in models [23,66]. From Table 4, the average yearly growth rate varies from 1.90 ppm year$^{-1}$ to 2.37 ppm year$^{-1}$ for GEOS-Chem and TCCON measurements during 2009–2011. The GEOS-Chem model shows a lower $XCO_2$ growth rate than those of TCCON sites.

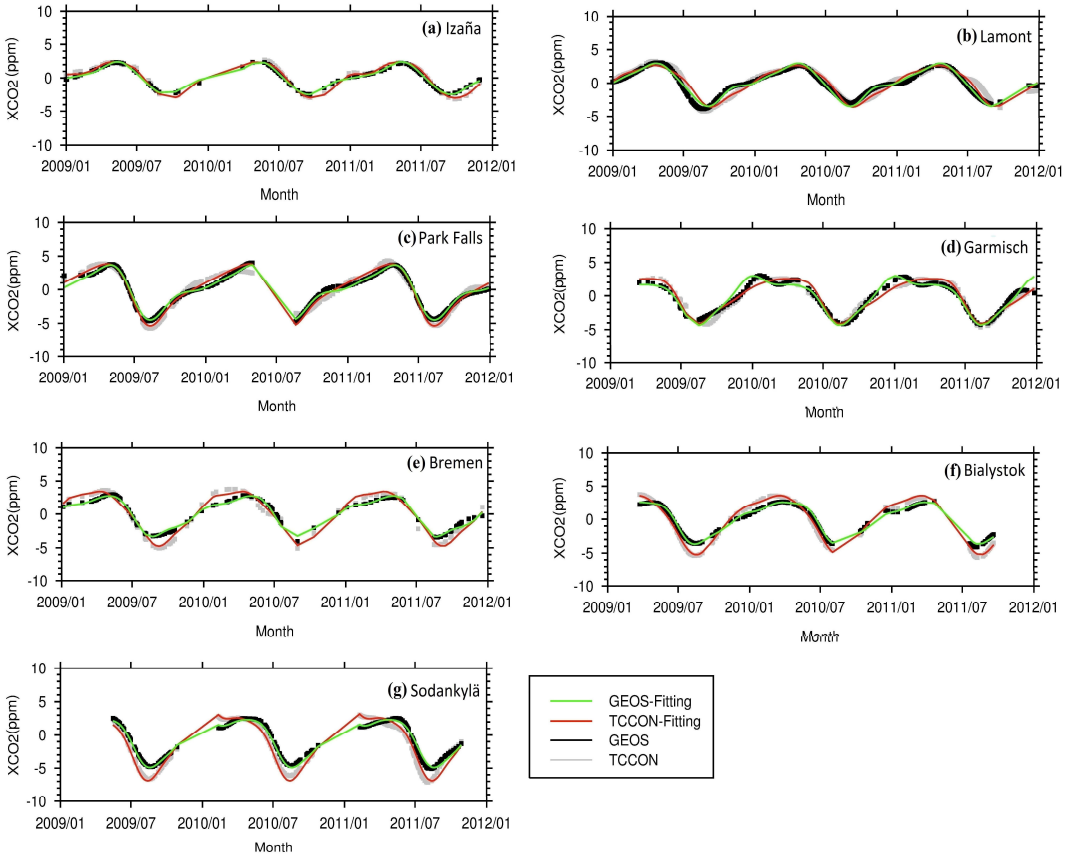


**Figure 12.** Seasonal cycles of $XCO_2$ are compared for GEOS-Chem and TCCON in the Northern Hemisphere during 2009–2011, which is calculated by removing the long-term trends of $XCO_2$ (gray dots for TCCON, black dots for GEOS-Chem); smoothed lines is fitting seasonal cycle (red for TCCON, green for GEOS-Chem).

**Table 4.** Comparison of the seasonal cycle amplitude and yearly growth rate between $XCO_2$ of GEOS-Chem and TCCON sites. Sites included Izaña, Lamont, Park Falls, Garmisch, Bremen, Bialystok, and Sodankylä.

| Sites | | Amplitude (ppm) | Growth Rate (ppm year$^{-1}$) | Period |
|---|---|---|---|---|
| Izaña | TCCON<br>GEOS | 5.29<br>4.96 | 2.24<br>2.01 | Jan/2009–Dec/2011 |
| Lamont | TCCON<br>GEOS | 6.52<br>6.35 | 2.37<br>2.09 | Jan/2009–Dec/2011 |
| Park Falls | TCCON<br>GEOS | 8.56<br>8.62 | 2.13<br>1.96 | Jan/2009–Dec/2011 |
| Garmisch | TCCON<br>GEOS | 6.9<br>7.1 | 1.89<br>1.82 | Sep/2009–Dec/2011 |
| Bremen | TCCON<br>GEOS | 8.8<br>6.9 | 2.29<br>1.91 | Jan/2009–Dec/2011 |
| Bialystok | TCCON<br>GEOS | 8.1<br>6.3 | 2.28<br>1.90 | Mar/2009–Sep/2011 |
| Sodankylä | TCCON<br>GEOS | 9.01<br>7.37 | 2.22<br>1.91 | May/2009–Oct/2011 |

We also investigate mean bias, RMSE and correlation coefficients between TCCON sites and GEOS-Chem as well as GOSAT/ACOS during April 2009–December 2011. Considering of $CO_2$ data availability at TCCON sites, only 9 TCCON sites including Bialystok, Bremen, Darwin, Garmisch, Lauder, Lamont, Orleans, Park Falls and Wollongong are used in this section. Similar to Cogan et al. [26], the averaging kernel and a priori have not been adopted in comparison between GOSAT/ACOS and TCCON sites, but they are used when comparing modeled $CO_2$ from GEOS-Chem with TCCON sites.

As shown by Figure 13, the overall correlations between $XCO_2$ from GEOS-Chem as well as GOSAT/ACOS and 9 TCCON sites are 0.93 and 0.74 respectively. The mean biases of $XCO_2$ is $-0.06$ ppm between GEOS-Chem and TCCON sites, and $-0.2$ ppm between GOSAT/ACOS and TCCON sites, and their RMSE is 1.19 ppm and 2.05 ppm respectively. The result show that the modeled $XCO_2$ from GEOS-Chem is underestimated on the whole by comparison with TCCON sites. Also, the result also indicate that $XCO_2$ retrievals from GOSAT/ACOSv7.3 show somewhat underestimated effect by comparison with TCCON sites, which may be due to retrieval errors or instrument issue of the GOSAT [23,26,68]. These results show good consistency with Section 4 and Cogan et al. [26].

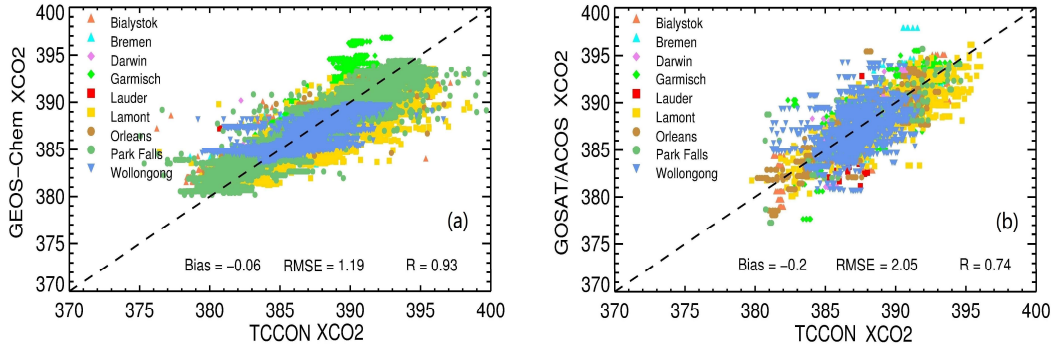


**Figure 13.** The scatter plot of $XCO_2$ between GEOS-Chem as well as GOSAT/ACOS and 9 TCCON sites during April 2009–December 2011. (**a**) The scatter plot between $XCO_2$ from GEOS-Chem and $XCO_2$ from TCCON sites; (**b**) The scatter plot between $XCO_2$ from GOSAT/ACOS and $XCO_2$ from TCCON sites.

## 5. Discussion

In this study, the comparison method mainly considered the averaging kernels among different $CO_2$ data according to Wunch et al. [28]. While horizontal $CO_2$ variability and differences in spatial support should be also considered in the future due to their impact in inter-comparison between different remote sensing observations [70]. For example, TCCON provide $XCO_2$ observations at a point location, and GOSAT/ACOS observation represents an average $XCO_2$ within the footprint 10.5 km in diameter [70]. The differences in spatial support may introduce another uncertainties when directly comparing between model results and observations [70]. Tadić and Michalak reported that different spatial support can lead to differences exceeding 0.5 ppm even for co-located $CO_2$ observations [70]. To roughly estimate the uncertainty raised from the spatial support, we compared the differences between the $XCO_2$ of GOSAT/ACOS (or TCCON sites) and the spatially averaged $XCO_2$ of GOSAT/ACOS (or TCCON sites) in a 2° × 2.5° grid which is in line with the horizontal resolution of GEOS-Chem $CO_2$ results.

From Figure 14, the differences (standard deviation) between GOSAT/ACOS $XCO_2$ observations and the corresponding averaged $XCO_2$ (at a 2° × 2.5° grid) ranged from 0–0.3 ppm and mostly distributed at 0–0.05 ppm. To some extent, these differences can be deemed as the impact of spatial support. To further understand the impact of averaged $XCO_2$ at 2° × 2.5° grids, we recalculated the correlation, averaged bias and RMSE between GOSAT/ACOS and GEOS-Chem at GOSAT footprint scale (using averaging kernels but no spatial support was considered) and 2° × 2.5° scales (using averaging kernels and then calculating the average), respectively, using data of 2010 on the global land. Table 5 shows that the correlation (R) is less affected by the effect of spatial support, while the mean bias and RMSE can be impacted by different spatial support.

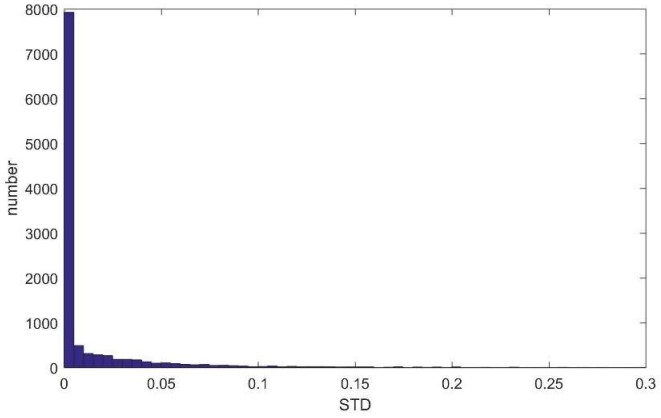


**Figure 14.** The frequency histogram of differences (standard deviations) between GOSAT $XCO_2$ and the corresponding averaged $XCO_2$ at 2° × 2.5° grids on the global land in 2010.

**Table 5.** Comparison between $XCO_2$ from GEOS-Chem and GOSAT/ACOS in 2010. It is noted that comparison of averaged $XCO_2$ between GEOS-Chem and GOSAT/ACOS observations at 2° × 2.5° grids was conducted after using averaging kernels.

| $XCO_2$ | R | Bias | RMSE |
|---|---|---|---|
| GEOS-Chem-ACOS (using averaging kernels and NO average) | 0.54 | 0.52 | 2.08 |
| GEOS-Chem-ACOS (using averaging kernels and then averaged) | 0.53 | 0.38 | 1.83 |

Similarly, 14 TCCON sites were also used to estimate the uncertainties of the spatial support and they include Lamont, Park Falls, Bialystok, Orleans, Garmisch, Bremen, Sodankylä, Ny-Ålesund,

Izaña, Eureka, Karlsruhe, Wollongong, Darwin, Lauder. From Figure 15, the differences (standard deviation) between $XCO_2$ at 14 TCCON sites and averaged $XCO_2$ at 2° × 2.5° grids mainly ranged from 0–1.4 ppm and mostly distributed at 0–0.1 ppm. This result indicates that different spatial support may bring relatively large uncertainties when directly comparing TCCON sites and GEOS-Chem.

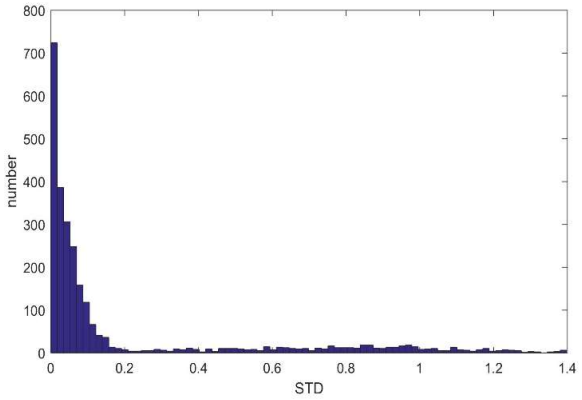


**Figure 15.** The frequency histogram of differences (standard deviations) between TCCON $XCO_2$ (14 sites) and the corresponding averaged $XCO_2$ in 2010 at 2° × 2.5° grids.

Also, the correlation, averaged bias and RMSE between $XCO_2$ from TCCON sites and GEOS-Chem in 2010 (Figure 16 and Table 6) were also calculated, which is similar to that of GOSAT/ACOS and GEOS-Chem. Similar to the comparison between GEOS-Chem and GOSAT, from Figure 16 and Table 6, we can see that the correlation is not affected by the spatial support, while the bias and RMSE is slightly affected.

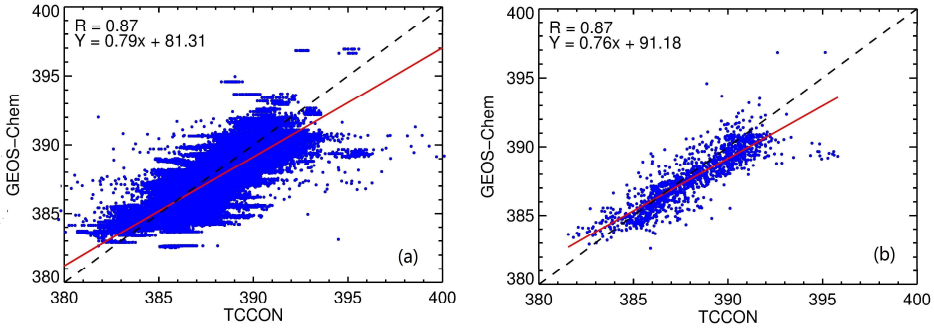


**Figure 16.** The scatter plots between $XCO_2$ from TCCON sites and GEOS-Chem ((**a**) using averaging kernels without considering the spatial support; (**b**) using averaging kernels and then calculating the average) in 2010.

**Table 6.** Comparison between $XCO_2$ from GEOS-Chem and TCCON sites in 2010.

| $XCO_2$ | R | Bias | RMSE |
|---|---|---|---|
| GEOS-Chem-TCCON (using averaging kernels and no average) | 0.87 | −0.41 | 1.06 |
| GEOS-Chem-TCCON (using averaging kernels and average) | 0.87 | −0.40 | 1.17 |

By comparing Figures 14 and 15, it is revealed that the impact of spatial support is more obvious for TCCON sites than that of GOSAT/ACOS measurements when comparing with GEOS-Chem results. This may be due to the spatial support of GOSAT/ACOS is more close to that of GEOS-Chem

than TCCON. Furthermore, the correlation analysis between GEOS-Chem and TCCON sites (or GOSAT/ACOS) indicates that the spatial support has no obvious effect on the correlation coefficient. However, the mean bias and RMSE is indeed influenced by spatial support. Therefore, the uncertainties from spatial support should be pay enough attention in the future, especially for comparison with TCCON $XCO_2$ point observations.

## 6. Conclusions

Global atmospheric $CO_2$ concentrations were effectively simulated by a global 3-D chemical transport model (GEOS-Chem) during the years of 2009–2011 and compared with $XCO_2$ data from the GOSAT satellite, CarbonTracker $CO_2$ modeling system and TCCON measurements in this study. The results indicate that the modeled $XCO_2$ from GEOS-Chem shows overall good consistency with GOSAT/ACOSv7.3, CarbonTracker, but the GEOS-Chem model overestimates $XCO_2$ values compared with the GOSAT/ACOSv7.3 $XCO_2$ retrievals at most regions, particularly in the SH and the high latitude of the NH.

The results also show that the monthly averaged $XCO_2$ of GEOS-Chem generally underestimate $XCO_2$ as compared to CarbonTracker, although they have a similar seasonal cycle. The discrepancies between the two models may be originated from a different transport model or the assimilation of observation in CarbonTracker. However, obvious overestimated $XCO_2$ from GEOS-Chem was found at the high latitudes of the Northern Hemisphere in JJA as compared with CarbonTracker or TCCON sites, which indicates that large uncertainties in GEOS-Chem over these regions probably because of the influences of atmospheric transport model and local flux. This phenomenon has been also reflected by comparison with GOSAT/ACOS.

Overall, although the simulated $CO_2$ from GEOS-Chem are in a good agreement with the GOSAT/ACOS retrievals, CarbonTracker and TCCON measurements, the discrepancies between them are considerable, e.g., the underestimation effect of $XCO_2$ in GEOS-Chem model, probably due to lack of constraints from measurements and affected by prior biosphere flux in model. Also, the obvious overestimated $XCO_2$ in the high latitude of the NH in JJA is needed to be concerned. Future work will need to assimilate observation data, e.g., GOSAT/ACOS or OCO-2, into the GEOS-Chem model to further optimize the $CO_2$ fluxes. These comparisons and analysis also indicated that GOSAT/ACOSv7.3 retrievals could underestimate the $XCO_2$. The uncertainties in satellite observations are necessary to quantify for further estimations of their assimilation into model systems. Furthermore, the uncertainties from spatial support should be carefully considered when inter-comparison among different observations and models.

**Author Contributions:** The work presented in this paper was carried out in a collaboration between all authors. The study was conceived by Y.J., T.W., P.Z., L.C., N.X. and Y.M. The writing was led by Y.J., T.W., P.Z., L.C., N.X. and Y.M. All authors contributed to reviewing and revising the text.

**Acknowledgments:** This work was supported by the National Natural Science Foundation of China (Grant No. 41475031, No. 41471304, No. 41571364 and No. 41771387) and China Postdoctoral Science Foundation (Grant No. 2016M590074).We acknowledge the ACOS/OCO-2 project at the Jet Propulsion Laboratory, California Institute of Technology and NASA Goddard Earth Science Data and Information Services Center for providing the ACOS7.3 $XCO_2$ data archive. CarbonTracker CT2013B results provided by NOAA ESRL, Boulder, Colorado, USA from the website at http://carbontracker.noaa.gov. In addition, TCCON data were obtained from the TCCON Data Archive, hosted by the Carbon Dioxide Information Analysis Center (CDIAC)—tccondata.org. We also thank David Griffith for his suggestion about the use of TCCON averaging kernels in comparison with GEOS-Chem model. We are also grateful for the GEOS-Chem model managed by the GEOS-Chem Support Team Support Team, based at Harvard University and Dalhousie University. Finally, we thanks for all reviewers for their comments about this manuscript, especially his/her suggestion about the uncertainties from spatial support.

**Conflicts of Interest:** The authors declare no conflict of interest.

## References


1. Intergovernmental Panel on Climate Change (IPCC). Summary for policymakers. In *Climate Change: The Physical Science Basis*; Contribution of Working Group I to the Fifth Assessment Report of the Intergovernmental Panel on Climate Change; Cambridge University Press: Cambridge, UK; New York, NY, USA, 2013.
2. Solomon, S.; Intergovernmental Panel on Climate Change; Intergovernmental Panel on Climate Change, Working Group I. *Climate Change 2007: The Physical Science Basis: Contribution of Working Group I to the Fourth Assessment Report of the Intergovernmental Panel on Climate Chang*; Cambridge University Press: Cambridge, UK; New York, NY, USA, 2007.
3. Shakun, J.D.; Clark, P.U.; He, F.; Marcott, S.A.; Mix, A.C.; Liu, Z.; Otto-Bliesner, B.; Schmittner, A.; Bard, E. Global warming preceded by increasing carbon dioxide concentrations during the last deglaciation. *Nature* **2012**, *484*, 49–54. [CrossRef] [PubMed]
4. Friedlingstein, P.; Cox, P.; Betts, R.; Bopp, L.; von Bloh, W.; Brovkin, V.; Cadule, P.; Doney, S.; Eby, M.; Fung, I.; et al. Climate-carbon cycle feedback analysis: Results from the C4MIP model intercomparison. *J. Clim.* **2006**, *19*, 3337–3353. [CrossRef]
5. Butz, A.; Hasekamp, O.P.; Frankenberg, C.; Aben, I. Retrievals of atmospheric $CO_2$ from simulated space-borne measurements of backscattered near-infrared sunlight: Accounting for aerosol effects. *Appl. Opt.* **2009**, *48*, 3322–3336. [CrossRef] [PubMed]
6. O'Dell, C.W.; Connor, B.; Bösch, H.; O'Brien, D.; Frankenberg, C.; Castano, R.; Christi, M.; Eldering, D.; Fisher, B.; Gunson, M.; et al. The ACOS $CO_2$ retrieval algorithm—Part 1: Description and validation against synthetic observations. *Atmos. Meas. Tech.* **2012**, *5*, 99–121. [CrossRef]
7. Reuter, M.; Buchwitz, M.; Schneising, O.; Heymann, J.; Bovensmann, H.; Burrows, J.P. A method for improved SCIAMACHY $CO_2$ retrieval in the presence of optically thin clouds. *Atmos. Meas. Tech.* **2010**, *3*, 209–232. [CrossRef]
8. Yokota, T.; Yoshida, Y.; Eguchi, N.; Ota, Y.; Tanaka, T.; Watanabe, H.; Maksyutov, S. Global Concentrations of $CO_2$ and $CH_4$ Retrieved from GOSAT: First Preliminary Results. *Sola* **2009**, *5*, 160–163. [CrossRef]
9. Frankenberg, C.; Pollock, R.; Lee, R.A.M.; Rosenberg, R.; Blavier, J.F.; Crisp, D.; O'Dell, C.W.; Osterman, G.B.; Roehl, C.; Wennberg, P.O.; et al. The Orbiting Carbon Observatory (OCO-2): Spectrometer performance evaluation using pre-launch direct sun measurements. *Atmos. Meas. Tech.* **2015**, *8*, 301–313. [CrossRef]
10. Chen, X.; Wang, J.; Liu, Y.; Xu, X.; Cai, Z.; Yang, D.; Yan, Y.; Feng, L. Angular dependence of aerosol information content in CAPI/TanSat observation over land: Effect of polarization and synergy with A-Train satellites. *Remote Sens. Environ.* **2017**, *196*, 163–177. [CrossRef]
11. Crisp, D.; Fisher, B.; O'Dell, C.; Frankenberg, C.; Basilio, R.; Bosch, H.; Brown, L.R.; Castano, R.; Connor, B.; Deutscher, N.M.; et al. The ACOS $CO_2$ retrieval algorithm—Part II: Global $XCO_2$ data characterization. *Atmos. Meas. Tech.* **2012**, *5*, 687–707. [CrossRef]
12. Wang, T.X.; Shi, J.C.; Jing, Y.Y.; Xie, Y.H. Investigation of the consistency of atmospheric $CO_2$ retrievals from different space-based sensors: Intercomparison and spatiotemporal analysis. *Chin. Sci. Bull.* **2013**, *58*, 4161–4170. [CrossRef]
13. Jing, Y.; Shi, J.; Wang, T.; Sussmann, R. Mapping Global Atmospheric $CO_2$ Concentration at High Spatiotemporal Resolution. *Atmosphere* **2014**, *5*, 870–888. [CrossRef]
14. Griffith, D.W.; Toon, G.C.; Connor, B.; Sussmann, R.; Warneke, T.; Deutscher, N.M.; Wennberg, P.O.; Notholt, J.; Sherlock, V.; Robinson, J.; et al. Preliminary validation of column-averaged volume mixing ratios of carbon dioxide and methane retrieved from GOSAT short-wavelength infrared spectra. *Atmos. Meas. Tech.* **2011**, *4*, 1061–1076. [CrossRef]
15. Zhang, H.; Chen, B.; Xu, G.; Yan, J.; Che, M.; Chen, J.; Fang, S.; Lin, X.; Sun, S. Comparing simulated atmospheric carbon dioxide concentration with GOSAT retrievals. *Chin. Sci. Bull.* **2015**, *60*, 380–386. [CrossRef]
16. Gurney, K.R.; Law, R.M.; Denning, A.S.; Rayner, P.J.; Baker, D.; Bousquet, P.; Bruhwiler, L.; Chen, Y.H.; Ciais, P.; Fan, S.; et al. TransCom 3 $CO_2$ inversion intercomparison: 1. Annual mean control results and sensitivity to transport and prior flux information. *Tellus B* **2003**, *55*, 555–579. [CrossRef]
17. Chevallier, F.; Feng, L.; Bösch, H.; Palmer, P.I.; Rayner, P.J. On the impact of transport model errors for the estimation of $CO_2$ surface fluxes from GOSAT observations. *Geophys. Res. Lett.* **2010**, *37*. [CrossRef]

18. Li, R.; Zhang, M.; Chen, L.; Kou, X.; Skorokhod, A. CMAQ simulation of atmospheric $CO_2$ concentration in East Asia: Comparison with GOSAT observations and ground measurements. *Atmos. Environ.* **2017**, *160*, 176–185. [CrossRef]
19. Lei, L.; Guan, X.; Zeng, Z.; Zhang, B.; Ru, F.; Bu, R. A comparison of atmospheric $CO_2$ concentration GOSAT-based observations and model simulations. *Sci. China Earth Sci.* **2014**, *57*, 1393–1402. [CrossRef]
20. Saito, R.; Patra, P.K.; Deutscher, N.; Wunch, D.; Ishijima, K.; Sherlock, V.; Blumenstock, T.; Dohe, S.; Griffith, D.; Hase, F.; et al. Latitude-time variations of atmospheric column-average dry air mole fractions of $CO_2$, $CH_4$ and $N_2O$. *Atmos. Chem. Phys.* **2012**, *12*, 7767–7777. [CrossRef]
21. Nassar, R.; Jones, D.B.; Suntharalingam, P.; Chen, J.M.; Andres, R.J.; Wecht, K.; Yantosca, R.M.; Kulawik, S.S.; Bowman, K.W.; Worden, J.R.; et al. Modeling Global Atmospheric $CO_2$ with Improved Emission Inventories and $CO_2$ Production from the Oxidation of Other Carbon Species. *Geosci. Model Dev.* **2010**, *3*, 689–716. [CrossRef]
22. Feng, L.; Palmer, P.I.; Yang, Y.; Yantosca, R.M.; Kawa, S.R.; Paris, J.D.; Matsueda, H.; Machida, T. Evaluating a 3-D transport model of atmospheric $CO_2$ using ground-based, aircraft, and space-borne data. *Atmos. Chem. Phys.* **2011**, *11*, 2789–2803. [CrossRef]
23. Lindqvist, H.; O'Dell, C.W.; Basu, S.; Boesch, H.; Chevallier, F.; Deutscher, N.; Feng, L.; Fisher, B.; Hase, F.; Inoue, M.; et al. Does GOSAT capture the true seasonal cycle of carbon dioxide. *Atmos. Chem. Phys.* **2015**, *15*, 13023–13040. [CrossRef]
24. Zhang, L.L.; Yue, T.X.; Wilson, J.P.; Zhao, N.; Zhao, Y.P.; Du, Z.P.; Liu, Y. A comparison of satellite observations with the $XCO_2$ surface obtained by fusing TCCON measurements and GEOS-Chem model outputs. *Sci. Total Environ.* **2017**, *601*, 1575–1590. [CrossRef] [PubMed]
25. Yoshida, Y.; Ota, Y.; Eguchi, N.; Kikuchi, N.; Nobuta, K.; Tran, H.; Morino, I.; Yokota, T. Retrieval algorithm for $CO_2$ and $CH_4$ column abundances from short-wavelength infrared spectral observations by the Greenhouse gases observing satellite. *Atmos. Meas. Tech.* **2011**, *4*, 717–734. [CrossRef]
26. Cogan, A.J.; Boesch, H.; Parker, R.J.; Feng, L.; Palmer, P.I.; Blavier, J.F.; Deutscher, N.M.; Macatangay, R.; Notholt, J.; Roehl, C.; et al. Atmospheric carbon dioxide retrieved from the Greenhouse gases Observing SATellite (GOSAT): Comparison with ground-based TCCON observations and GEOS-Chem model calculations. *J. Geophys. Res. Atmos.* **2012**, *117*. [CrossRef]
27. Osterman, G.; Eldering, A.; Cheng, C.; O'Dell, C.; Martinez, E.; Crisp, D.; Frankenberg, C.; Fisher, B.; Wunch, D. *ACOS Level 2 Standard Product and Lite Data Product Data User's Guide, v7.3*; GES DISC: Greenbelt, MD, USA, 2017.
28. Wunch, D.; Toon, G.C. Calibration of the Total Carbon column Observing Network using aircraft profile data. *Atmos. Meas. Tech.* **2010**, *3*, 1351–1362. [CrossRef]
29. Wunch, D.; Toon, G.C.; Blavier, J.-F.L.; Washenfelder, R.A.; Notholt, J.; Connor, B.J.; Griffith, D.W.T.; Sherlock, V.; Wennberg, P.O. The Total Carbon Column Observing Network. *Philos. Trans. R. Soc. A Math. Phys. Eng. Sci.* **2011**, *369*, 2087–2112. [CrossRef] [PubMed]
30. Messerschmidt, J.; Geibel, M.C.; Blumenstock, T.; Chen, H.; Deutscher, N.M.; Engel, A.; Feist, D.G.; Gerbig, C.; Gisi, M.; Hase, F.; et al. Calibration of TCCON column-averaged $CO_2$: The first aircraft campaign over European TCCON sites. *Atmos. Chem. Phys.* **2011**, *11*, 10765–10777. [CrossRef]
31. Wennberg, P.O.; Wunch, D.; Roehl, C.; Blavier, J.-F.; Toon, G.C.; Allen, N.; Dowell, P.; Teske, K.; Martin, C.; Martin, J. *TCCON Data from Lamont, Oklahoma, USA, Release GGG2014.R1. TCCON Data Archive, Hosted by the Carbon Dioxide Information Analysis Center, Oak Ridge National Laboratory, Oak Ridge, Tennessee, U.S.A.*; Oak Ridge National Laboratory: Oak Ridge, TN, USA, 2016. [CrossRef]
32. Wennberg, P.O.; Roehl, C.; Wunch, D.; Toon, G.C.; Blavier, J.-F.; Washenfelder, R.; Keppel-Aleks, G.; Allen, N.; Ayers, J. *TCCON Data from Park Falls, Wisconsin, USA, Release GGG2014R0. TCCON Data Archive, Hosted by the Carbon Dioxide Information Analysis Center, Oak Ridge National Laboratory, Oak Ridge, Tennessee, U.S.A.*; Oak Ridge National Laboratory: Oak Ridge, TN, USA, 2014. [CrossRef]
33. Washenfelder, R.A.; Toon, G.C.; Blavier, J.F.; Yang, Z.; Allen, N.T.; Wennberg, P.O.; Vay, S.A.; Matross, D.M.; Daube, B.C. Carbon dioxide column abundances at the Wisconsin Tall Tower site. *J. Geophys. Res. Atmos.* **2006**, *111*, D22305. [CrossRef]

34. Deutscher, N.; Notholt, J.; Messerschmidt, J.; Weinzierl, C.; Warneke, T.; Petri, C.; Grupe, P.; Katrynski, K. *TCCON Data from Bialystok, Poland, Release GGG2014R1. TCCON Data Archive, Hosted by the Carbon Dioxide Information Analysis Center, Oak Ridge National Laboratory, Oak Ridge, Tennessee, U.S.A.*; Oak Ridge National Laboratory: Oak Ridge, TN, USA, 2015. [CrossRef]
35. Messerschmidt, J.; Chen, H.; Deutscher, N.M.; Gerbig, C.; Grupe, P.; Katrynski, K.; Koch, F.T.; Lavrič, J.V.; Notholt, J.; Rödenbeck, C.; et al. Automated ground-based remote sensing measurements of greenhouse gases at the Białystok site in comparison with collocated in situ measurements and model data. *Atmos. Chem. Phys.* **2012**, *12*, 6741–6755. [CrossRef]
36. Warneke, T.; Messerschmidt, J.; Notholt, J.; Weinzierl, C.; Deutscher, N.; Petri, C.; Grupe, P.; Vuillemin, C.; Truong, F.; Schmidt, M.; et al. *TCCON Data from Orleans, France, Release GGG2014R0. TCCON Data Archive, Hosted by the Carbon Dioxide Information Analysis Center, Oak Ridge National Laboratory, Oak Ridge, Tennessee, U.S.A.*; Oak Ridge National Laboratory: Oak Ridge, TN, USA, 2014. [CrossRef]
37. Messerschmidt, J.; Macatangay, R.; Notholt, J.; Petri, C.; Warneke, T.; Weinzierl, C. Side by side measurements of $CO_2$ by ground-based Fourier transform spectrometry (FTS). *Tellus B* **2010**, *62*, 749–758. [CrossRef]
38. Sussmann, R.; Rettinger, M. *TCCON Data from Garmisch, Germany, Release GGG2014R0.TCCON Data Archive, Hosted by the Carbon Dioxide Information Analysis Center, Oak Ridge National Laboratory, Oak Ridge, Tennessee, U.S.A.*; Oak Ridge National Laboratory: Oak Ridge, TN, USA, 2014. [CrossRef]
39. Hausmann, P.; Sussmann, R.; Smale, D. Contribution of oil and natural gas production to renewed increase in atmospheric methane (2007–2014): Top–down estimate from ethane and methane column observations. *Atmos. Chem. Phys.* **2016**, *16*, 3227–3244. [CrossRef]
40. Notholt, J.; Petri, C.; Warneke, T.; Deutscher, N.; Buschmann, M.; Weinzierl, C.; Macatangay, R.; Grupe, P. *TCCON Data from Bremen, Germany, Release GGG2014R0. TCCON Data Archive, Hosted by the Carbon Dioxide Information Analysis Center, Oak Ridge National Laboratory, Oak Ridge, Tennessee, U.S.A.*; Oak Ridge National Laboratory: Oak Ridge, TN, USA, 2014. [CrossRef]
41. Kivi, R.; Heikkinen, P.; Kyro, E. *TCCON Data from Sodankyla, Finland, Release GGG2014R0. TCCON Data Archive, Hosted by the Carbon Dioxide Information Analysis Center, Oak Ridge National Laboratory, Oak Ridge, Tennessee, U.S.A.*; Oak Ridge National Laboratory: Oak Ridge, TN, USA, 2014. [CrossRef]
42. Kivi, R.; Heikkinen, P. Fourier transform spectrometer measurements of column $CO_2$ at Sodankylä, Finland. *Geosci. Instrum. Methods Data Syst.* **2016**, *5*, 271–279. [CrossRef]
43. Blumenstock, T.; Hase, F.; Schneider, M.; Garcia, O.E.; Sepulveda, E. *TCCON Data from Izana, Tenerife, Spain, Release GGG2014R0. TCCON Data Archive, Hosted by the Carbon Dioxide Information Analysis Center, Oak Ridge National Laboratory, Oak Ridge, Tennessee, U.S.A.*; Oak Ridge National Laboratory: Oak Ridge, TN, USA, 2014. [CrossRef]
44. Strong, K.; Mendonca, J.; Weaver, D.; Fogal, P.; Drummond, J.R.; Batchelor, R.; Lindenmaier, R. *TCCON Data from Eureka, Canada, Release GGG2014R0. TCCON Data Archive, Hosted by the Carbon Dioxide Information Analysis Center, Oak Ridge National Laboratory, Oak Ridge, Tennessee, U.S.A.*; Oak Ridge National Laboratory: Oak Ridge, TN, USA, 2016. [CrossRef]
45. Hase, F.; Blumenstock, T.; Dohe, S.; Gross, J.; Kiel, M. *TCCON Data from Karlsruhe, Germany, Release GGG2014R1. TCCON Data Archive, Hosted by the Carbon Dioxide Information Analysis Center, Oak Ridge National Laboratory, Oak Ridge, Tennessee, U.S.A.*; Oak Ridge National Laboratory: Oak Ridge, TN, USA, 2015. [CrossRef]
46. Griffith, D.W.T.; Velazco, V.A.; Deutscher, N.; Murphy, C.; Jones, N.; Wilson, S.; Macatangay, R.; Kettlewell, G.; Buchholz, R.R.; Riggenbach, M. *TCCON Data from Wollongong, Australia, Release GGG2014R0. TCCON Data Archive, Hosted by the Carbon Dioxide Information Analysis Center, Oak Ridge National Laboratory, Oak Ridge, Tennessee, U.S.A.*; Oak Ridge National Laboratory: Oak Ridge, TN, USA, 2014. [CrossRef]
47. Griffith, D.W.T.; Deutscher, N.; Velazco, V.A.; Wennberg, P.O.; Yavin, Y.; Aleks, G.; Washenfelder, R.; Toon, G.C.; Blavier, J.-F.; Murphy, C.; et al. *TCCON Data from Darwin, Australia, Release GGG2014R0. TCCON Data Archive, Hosted by the Carbon Dioxide Information Analysis Center, Oak Ridge National Laboratory, Oak Ridge, Tennessee, U.S.A.*; Oak Ridge National Laboratory: Oak Ridge, TN, USA, 2014. [CrossRef]
48. Deutscher, N.; Griffith, D.; Bryant, G.; Wennberg, P.; Toon, G.; Washenfelder, R.; Keppel-Aleks, G.; Wunch, D.; Yavin, Y.; Allen, N.; et al. Total column $CO_2$ measurements at Darwin, Australia-site description and calibration against in situ aircraft profiles. *Atmos. Meas. Tech.* **2010**, *3*, 947–958. [CrossRef]

49. Sherlock, V.; Connor, B.; Robinson, J.; Shiona, H.; Smale, D.; Pollard, D. *TCCON Data Archive, Hosted by the Carbon Dioxide Information Analysis Center, Oak Ridge National Laboratory, Oak Ridge, Tennessee, U.S.A.*; Oak Ridge National Laboratory: Oak Ridge, TN, USA, 2014. [CrossRef]
50. Bey, I.; Jacob, D.J.; Yantosca, R.M.; Logan, J.A.; Field, B.D.; Fiore, A.M.; Li, Q.; Liu, H.Y.; Mickley, L.J.; et al. Global modeling of tropospheric chemistry with assimilated meteorology: Model description and evaluation. *J. Geophys. Res. Atmos.* **2001**, *106*, 23073–23095. [CrossRef]
51. Suntharalingam, P.; Jacob, D.J.; Palmer, P.I.; Logan, J.A.; Yantosca, R.M.; Xiao, Y.; Evans, M.J.; Streets, D.; Vay, S.A.; Sachse, G. Improved quantification of Chinese carbon fluxes using $CO_2$/CO correlations in Asian outflow. *J. Geophys. Res.* **2004**, *109*. [CrossRef]
52. Andres, R.J.; Gregg, J.S.; Losey, L.; Marland, G.; Boden, T.A. Monthly, global emissions of carbon dioxide from fossil fuel consumption. *Tellus B* **2011**, *63*, 309–327. [CrossRef]
53. Van der Werf, G.R.; Randerson, J.T.; Giglio, L.; Collatz, G.J.; Mu, M.; Kasibhatala, P.S.; Morton, D.C.; DeFries, R.S.; Jin, Y.; van Leeuwen, T.T. Global fire emissions and the contribution of deforestation, savanna, forest, agricultural, and peat fires (1997–2009). *Atmos. Chem. Phys.* **2010**, *10*, 11707–11735. [CrossRef]
54. Olsen, S.C.; Randerson, J.T. Differences between surface and column atmospheric $CO_2$ and implications for carbon cycle research. *J. Geophys. Res. Atmos.* **2004**, *109*. [CrossRef]
55. Baker, D.F.; Law, R.M.; Gurney, K.R.; Rayner, P.; Peylin, P.; Denning, A.S.; Bousquet, P.; Bruhwiler, L.; Chen, Y.H.; Ciais, P.; et al. TransCom 3 inversion intercomparison: Impact of transport model errors on the interannual variability of regional $CO_2$ fluxes, 1988–2003. *Glob. Biogeochem. Cycles* **2006**, *20*. [CrossRef]
56. Takahashi, T.; Sutherland, S.C.; Wanninkhof, R.; Sweeney, C.; Feely, R.A.; Chipman, D.W.; Hales, B.; Friederich, G.; Chavez, F.; Sabine, C.; et al. Climatological mean and decadal change in surface ocean $pCO_2$, and net sea-air $CO_2$ flux over the global oceans. *Deep Sea Res. Part II Top. Stud. Oceanogr.* **2009**, *56*, 2075–2076. [CrossRef]
57. Peters, W.; Jacobson, A.R.; Sweeney, C.; Andrews, A.E.; Conway, T.J.; Masarie, K.; Miller, J.B.; Bruhwiler, L.M.P.; Petron, G.; Hirsch, A.I.; et al. An atmospheric perspective on North America carbon dioxide exchange: Carbon Tracker. *Proc. Natl. Acad. Sci. USA* **2007**, *104*, 18925–18930. [CrossRef] [PubMed]
58. CarbonTracker Site. Available online: www.esrl.noaa.gov/gmd/ccgg/carbontracker (accessed on 25 June 2017).
59. CarbonTracker Document. CarbonTracker 2013-ESRL Global Monitoring Division, CarbonTracker Team: Boulder, Colorado, USA, 2015.
60. Jacobson, A.R.; Gruber, N.; Sarmiento, J.L.; Gloor, M.; Mikaloff Fletcher, S.E. A joint atmosphere-ocean inversion for surface fluxes of carbon dioxide: I. Methods and global-scale fluxes. *Glob. Biogeochem. Cycles* **2007**, *21*. [CrossRef]
61. Rodgers, C.D.; Connor, B.J. Intercomparison of remote sounding instruments. *J. Geophys. Res. Atmos.* **2003**, *108*. [CrossRef]
62. Toon, G.C.; Wunch, D. *TCCON Data Archive, Hosted by the Carbon Dioxide Information Analysis Center, Oak Ridge National Laboratory, Oak Ridge, Tennessee, U.S.A. TCCON Data Archive, Hosted by the Carbon Dioxide Information Analysis Center, Oak Ridge National Laboratory, Oak Ridge, Tennessee, U.S.A.*; Oak Ridge National Laboratory: Oak Ridge, TN, USA, 2014. [CrossRef]
63. Wunch, D.; Toon, G.C.; Sherlock, V.; Deutscher, N.M.; Liu, C.; Feist, D.G.; Wennberg, P.O. *The Total Carbon Column Observing Network's GGG2014 Data Version. Technical report, Carbon Dioxide Information Analysis Center, Oak Ridge National Laboratory, Oak Ridge, Tennessee, U.S.A.*; Oak Ridge National Laboratory: Oak Ridge, TN, USA, 2015. [CrossRef]
64. Miao, R.; Lu, N.; Yao, L.; Zhu, Y.; Wang, J.; Sun, J. Multi-year comparison of carbon dioxide from satellite data with ground-based FTS measurements (2003–2011). *Remote Sens.* **2013**, *5*, 3431–3456. [CrossRef]
65. Hammerling, D.M.; Michalak, A.M.; O'Dell, C.; Kawa, S.R. Global $CO_2$ distributions over land from the Greenhouse Gases Observing Satellite (GOSAT). *Geophys. Res. Lett.* **2012**, *39*. [CrossRef]
66. Basu, S.; Houweling, S.; Peters, W.; Sweeney, C.; Machida, T.; Maksyutov, S.; Patra, P.K.; Saito, R.; Chevallier, F.; Niwa, Y.; et al. The seasonal cycle amplitude of total column $CO_2$: Factors behind the model-observation mismatch. *J. Geophys. Res. Atmos.* **2011**, *116*. [CrossRef]
67. Belikov, D.A.; Maksyutov, S.; Sherlock, V.; Aoki, S.; Deutscher, N.M.; Dohe, S.; Griffith, D.; Kyro, E.; Morino, I.; Nakazawa, T.; et al. Simulations of column-averaged $CO_2$ and $CH_4$ using the NIES TM with a hybrid sigma-isentropic (σ-θ) vertical coordinate. *Atmos. Chem. Phys.* **2013**, *13*, 1713–1732. [CrossRef]

68. Kulawik, S.; Wunch, D.; O'Dell, C.; Frankenberg, C.; Reuter, M.; Oda, T.; Chevallier, F.; Sherlock, V.; Buchwitz, M.; Osterman, G.; et al. Consistent evaluation of GOSAT, SCIAMACHY, CarbonTracker, and MACC through comparisons to TCCON. *Atmos. Meas. Tech.* **2016**, *9*, 683–709. [CrossRef]
69. Thoning, K.W.; Tans, P.P.; Komhyr, W.D. Atmospheric carbon dioxide at Mauna Loa Observatory: 2. Analysis of the NOAA GMCC data, 1974–1985. *J. Geophys. Res. Atmos.* **1989**, *94*, 8549–8565. [CrossRef]
70. Tadić, J.M.; Michalak, A.M. On the effect of spatial variability and support on validation of remote sensing observations of $CO_2$. *Atmos. Environ.* **2016**, *132*, 309–316. [CrossRef]